UNIVERSITY of RWANDA

COLLEGE OF SCIENCE AND TECHNOLOGY

PREDICTING THE FUTURE VEGETATION COVER IN RESPONSE TO CLIMATE CHANGE IN RWANDA

By

MUSHIMIYIMANA Viateur

Registration number: 221027592

A dissertation submitted in partial fulfillment of the requirements for the degree of MASTER OF SCIENCE IN ATMOSPHERIC AND CLIMATE SCIENCE in the College of Science and Technology

Supervisor: Prof. Bonfils SAFARI

Co-supervisor: Dr. Deogratias NTIRIKWENDERA

October 2024

DECLARATION

I declare that this Dissertation embeds my own work except where specifically acknowledged, and it has been passed through the anti-plagiarism system and found to be compliant and this is the approved final version of the Thesis:

MUSHIMIYIMANA Viateur

Reg:221027592

Signed……..

Date……..

CERTIFICATION

This is to certify that the master's dissertation entitled "**Predicting the future vegetation cover in response to climate change in Rwanda**" was carried out by MUSHIMIYIMANA Viateur in partial fulfillment of the requirement for the Award of Master's Degree in Atmospheric and climate science in University of Rwanda, College of Science and Technology.

Supervisor:

Prof. Bonfils SAFARI

Date: ……../……./2024

Head of Physics Department:

Dr. Innocent NKURIKIYIMFURA

Date:……/…./2024

Dean of the School of Science

Prof. Denis NDANGUZA

Date: ……../……/2024

DEDICATION

This work is dedicated to my wife KAMUZIMA Beatrice, daughters SHIMWA Alta Vera, SENGA Anice Lita, son IZERA Jed Wise, my parents, and all my relatives.

ACKNOWLEDGEMENT

My highest gratitude is attributed to Almighty God for strengthening me during my studies in this program at the University of Rwanda.

I thank the University of Rwanda, College of Science and Technology for allowing me the admission to follow the Master's program in Atmospheric and Climate Science.

I considerably appreciate the great contribution of my supervisor Prof. Bonfils SAFARI and co-supervisor Dr. Deogratias NTIRIKWENDERA to the completion of this work.

I express my appreciation to all my lecturers who contributed to my knowledge improvement in the field of atmospheric and climate sciences. May the Lord rise the outcomes of your talented efforts.

May God bless my wife and children as well as all members of my extended family for their incentive advice that helped me to reach this very interesting step.

My thanks are to Mr. SEBAZIGA NDAKIZE Joseph and Mr. KAGABO SAFARI Abdou as well as RWEMA Michel for the voluntary technical support they allowed me during this research. May God bless you and ,yours very much.

I express also good wishes to my classmates for their collaboration and positive interaction during our studies.

Last but not least, I am delighted to thank Meteo Rwanda institution for giving me meteo stations data that have been used in this research.

ABSTRACT

Climate change, one of the global main threats brings about environmental fluctuations including the vegetation cover change in an area. This study concerns the response of vegetation cover to climate change in Rwanda for the period of 2024 to 2053. The Normalized Difference Vegetation Index (NDVI) was used to monitor the vegetation cover status in terms of the temperature and rainfall in Rwanda. MPI-REMO inputted by two Representative Concentration Pathways: RCP 2.6 and RCP 8.5 was used to predict the Normalized Difference Vegetation Index (NDVI) in 2024-2053.

The results showed that the annual change in rainfall from 1983 to 2020 was approximately $0.7mm$ and the mean temperature was approximately $0.2°C$**.** The grasslands as well as the shrubs governed many regions in the study area from 1983 to 2020 and NDVI will increase from the North to South and from East to West of the study area under the scenarios in consideration during the 2024 -2053 period. The NDVI will increase with the slope of $0.0009year^{-1}$and $0.0002year^{-1}$at the high emission and low emission respectively during the 2043-2053 period. The correlation of NDVI to either rainfall or mean temperature was unequally distributed in the study area with a low positive or negative coefficient of correlation**.** However**,** the NDVI was more correlated to mean temperature than rainfall in different regions of the study area during the 1983-2020 period. This will be the same under the two scenarios in consideration during the 2024-2053 period. To implement the conservation strategies of a green environment in Rwanda, one should take into account the factors enhancing climate change such as the greenhouse gas emissions in the atmosphere training without ceasing the mitigation measures.

LIST OF SYMBOLS AND ACRONYMS

AVHRR: Advanced Very-High-Resolution Radiometer

CO_2: carbon dioxide:

CDO: Climate Data Operator

CDR: Climate Data Record

CDT: Climate Data Tool

CORDEX: Coordinated Regional Downscaling Experiment

CSC: Climate System Center

CV: Coefficient of Variation

DJF: December, January and February

ENACTS: Enhancing National Climate Services

EN: El Niño

ENSO: El Niño Southern Oscillation

eq: equivalent

ESGF: Earth's System Grid Federation

EVI: Enhanced Vegetation Index

GCMs: Global Circulations Models

GIS: Geographic Information System

GVI: Green Vegetation Index

IDW: Inverse Distance Weighting,

IPCC: Intergovernmental Panel on Climate Change:

ITCZ: Inter-Tropical Convergence Zone

JJA: June, July and August

LAI: Leaf Area Index

MAE: Mean Absolute Error

MAM: March, April, May

MK: Mann-Kendal

MPI-ESM-LR: Max Planck Institute for Meteorology's Earth System Model at low resolution

MPI-REMO: Max Planck Institute Regional Model

ppm: parts per million

NDVI: Normalized Difference Vegetation Index

NIR: Near-infrared

NOAA-7: National Oceanic and Atmospheric Administration version 7

REMO: Regional Model

RCM: Regional Climate Models

RCP: Representative Concentration Pathway

RPHC5: Fifth Rwanda Population and Housing Census

RVI: Ratio Vegetation Index

SO: Southern Oscillation

SON: September, October, November

SOND: September-October-November-December

SST: Sea-Surface Temperature

St: Saint

TABLE OF CONTENT

LIST OF FIGURES

LIST OF TABLES

CHAPTER ONE: INTRODUCTION

1.1. Background

Global climate change has become real and evident and is now among the most threatening issues in the world. Climate change is defined, according to the Intergovernmental Panel on Climate Change (IPCC) as a change in the state of the climate that can be identified by changes in mean and/or the variability of its properties and that persists for an extended period, typically decades or longer [1]**.** Climate change is enhanced by the increase in atmospheric carbon dioxide (CO_2) concentrations due to human- made activities[2] and its reality is observed through different variables principally variability in temperature and rainfall which lead to extreme events such as floods, droughts, and landslides.

Climate change and human-made activities have caused environmental and ecosystem degradation in Rwanda. For example, the climate change-based threat brought Rwanda's natural forest reduction as well as its dwelling biodiversity since the 1970s [3]**.**

Vegetation cover is one of the very important components of terrestrial ecosystems. Different researchers took advantage to study how the vegetation cover is monitored by climate change using the remote sensing Normalized Difference Vegetation Index (NDVI) resources and the climate variables such as temperature and rainfall. For example, [4] has shown that precipitation is one of the principal factors that determine the vegetation dynamics in Xinjiang, China. [5]found precipitation and air temperature to be the two most important meteorological elements that influence the dynamic change of land vegetation in Chinese mainland regions. Statistical analysis revealed a positive correlation between mean NDVI and precipitation as well as with surface temperature for different kinds of vegetation in Rwanda [6].

The effective protection of the environment as well as the repair of ecology result from tracking and forecasting the vegetation cover [7]**.** It was predicted that the mean monthly temperature in Rwanda will increase by 1.7-2.2^{o}C by 2050 compared to the historical mean monthly temperature during the period of 1980 to 2010 while the total annual precipitation will be reduced during the same period in all country provinces (https://bit.ly/3UMwdxl).

It is therefore of great importance to investigate how the future climate change will affect the vegetation as this later is the very life-dependent element in Rwanda.

1.2. Problem statement

Vegetation cover plays a big role in biodiversity well-being but has experienced significant degradation for years ago [8],[9]. Different researchers such as[10], [11], and [12] found that the rainfall and temperature have been changing, but they did not apply these changes to the vegetation cover variations in Rwanda. However, both rainfall and temperature changes as some of the events triggered by climate change also influence the vegetation cover [13]. Few studies were conducted on the contribution of climate change to the vegetation cover in Rwanda [6],[14]. In addition, the conducted works did not come to the behavior of the vegetation cover in reaction to the climate change for the future decades in Rwanda while the future climate change is projected.

Therefore, there is an insistent need to predict the future vegetation cover in response to climate change in Rwanda. The study will develop serviceable strategies for policymakers to be more informed in decision-making on a sustainable country's natural resources, particularly vegetation cover.

1.3. Objectives

The overall objective of this study is to predict the future vegetation cover in response to climate change in RWANDA. The specific objectives that are set to achieve the main objective are the following:

1. Analyze the variability of rainfall, temperature, and vegetation cover in Rwanda during the period from 1983 to 2020.
2. Determine the relationship between the vegetation cover and both rainfall and temperature.
3. Elucidate how the vegetation cover will change for the period between 2024 and 2053**.**

1.4. Hypothesis of the study

Although the vegetation cover in Rwanda is influenced by direct anthropogenic activities, its nature, type, and distribution are also highly influenced by climate. We premise that the variability in rainfall and temperature in Rwanda will bring about vegetation changes where the change will depend on the regions and time scale considered.

1.5. Justification of the study

Principal environmental key issues facing Rwanda include climate change which brings about biodiversity loss and vegetation cover in turn [15]. Sufficient information on how climate change affects vegetation is needed for the sustainable conservation of the environment. The results will grasp the interdependence of vegetation variation and variability of temperature and rainfall, and this shall give insight to the strategic planners and implementers on a clear basis for environmental restoration and/or protection policies in Rwanda for the future decades.

1.6. Study area

1.6.1. Administrative structure of Rwanda

Rwanda, also called the country of a "thousand hills'' because of its elevated hilly relief, is an East African country that is near the Equator and is still developing. It is between latitudes of 1°04' and 2°51' South and longitudes of 28°53' and 30°53' East [16]. Rwanda has a surface area of 26 338 square kilometers. It is subdivided into five Provinces which are Northern Province, Southern Province, Eastern Province, Western Province, and Kigali City (**Figure 1**). The fifth Rwanda Population and Housing Census (RPHC5) done in 2022 indicates that the population of Rwanda is about 13 246 394 persons, that is, the density of 503 inhabitants per square kilometer(https://bit.ly/3U38hpA). The bordering countries of Rwanda are Uganda in the North, Burundi in the South, Tanzania in the East, and the Democratic Republic of Congo in the West. Rwanda counts four national parks which are the Akagera National Park, Nyungwe National Park, and the Volcanoes National Park.

1.6.2. Climate of Rwanda

Even if it is near the equator, Rwanda is not in an equatorial climate. It has a temperate climate instead [3]. Being in a tropical temperate climate, Rwanda's average annual temperature is between 15 and 17°C in the highland area,18°C and 20°C in the Central Plateau, and more than 24°C in eastern lowlands and the southwestern region near Bugarama**.** Whereas the rainfall ranges from about 900 mm in the east and southeast parts of Eastern lowlands, it is around 1500 mm in the north and northwest volcanic highland areas and around 1200 mm in the area of Central Plateau. The wind speed turns around 1 to 3m/s [16],[17].

The temperate climate of Rwanda consists of relief that is dominantly hilly, mountainous, and with plateaus. It includes inadequate forests, few wetlands, and large water bodies and is affected by human activities. Rwanda's climate is in four climatic zones which are the lowlands of Eastern Province, the central plateau, the highlands of Gicumbi, Congo Nile crest and Birunga regions, the plains of Bugarama, and the Lake Kivu as well as its surroundings areas (https://bit.ly/4b1gali).

Rwanda presents four seasons characterizing rainfall distribution which are short rainy season locally known as *Umuhindo* comprising months of September, October, and November (SON; the short dry season locally known as *Urugaryi* which takes place during December, January, and February (DJF longer rainy season locally known as *Itumba* which is during March, April, and May (MAM) and larger dry season known under the name of *Icyi* ranging from June to August, that is June, July and August (JJA Eastern and southeastern regions in Rwanda more suffer greatly from prolonged droughts.

1.6.2.1. Drivers of Rwanda's climate

The climate of Rwanda is so important to Rwanda's development as its economy is significantly dependent on rain-yielded agriculture. The main drivers of Rwanda's climate include the altitude or topography, the regional atmospheric circulations mainly the Inter-Tropical Convergence Zone (ITCZ), ENSO, the subtropical anticyclones, tropical cyclones, monsoons, Easterly waves, and so on[18], [19].

Rwanda's altitude.

Due to its high elevation, Rwanda is placed in a temperate climate and the Albertine branch of the Rift Valley that extends to the western part of Rwanda makes this region mountainous and with altitudes approximately over 2000m above sea level. These heights lower into the range of 1500m through 2000m towards the central plateau and less than 1500m in the eastern region towards the border with Tanzania [20]. The orographic motions determine the amount of rainfall in the two long rain seasons of MAM(March-April-May) and SOND (September-October-November-December) in Rwanda as these motions are influenced according to Rwanda's topography [21]. The complex topography of Rwanda is a factor playing a big role in Rwanda's average temperature variation. The country's high altitudes in Rwanda moderate the temperatures where these later are lower than in equatorial regions. In highland regions, one has low temperatures with average temperatures ranging between 15 and 17°C. Moderate temperatures are found to be between 19 and 21°C.In the East and Southwest of the country consisting of lowlands temperatures are higher and the extreme can go beyond 30°C in February and July-August [16].

Inter-Tropical Convergence Zone (ITCZ)

The Inter-Tropical Convergence Zone refers to the region where the northeasterly trade winds that come from the Northern Hemisphere converge together with the southeasterly trade winds from the Southern Hemisphere[22]. This band characterized by low pressure, maximum humidity, and convergence of winds is also called "climate equator" and shifts north and south of the equator with the changing seasons. In East Africa, the Inter-Tropical Convergence Zone moves northward from February to May, and southward from October to December. Due to the ITCZ's large-coved distance, the East African regions experience rain seasons with less intensity than the Western region of Africa [23]. As in other countries in East Africa, the rainfall distribution over Rwanda is also driven by the Inter-Tropical Convergence Zone[21].

Under control of the subtropical anticyclone's intensity and position, the Intertropical Convergence Zone (ITCZ) governs the climate of Rwanda as it passes twice a year in the country generating two rain seasons which take place from mid-September to mid-December and from March to May [24]. Whereas the MAM rainy season presents itself when ITCZ converges from the south to the north hemisphere, the SOND rainy season takes place when it migrates from the north to the south hemisphere. The rainfall is northwest-east allotted, giving more rainfall in

the northwestern than the eastern part of Rwanda[25].In general, the Intertropical Convergence Zone (ITCZ) induces the humidified winds from the Indian Ocean and Lake Victoria generating the rain season from mid-September to mid-December (SOND). The Dry season from mid-December to the end of February is caused by the dry and cold East Africa air masses from Arabian Dorsal as induced also by ITCZ. The rain season that takes place from March to May (MAM) originates from the ITCZ-induced South easterly and south-westerly dry wind carrying humidity from the South Atlantic passing through the Congo Basin. The dry season from June to September, is caused by ITCZ-induced continental dry South Easterly winds crossing Tanzania to Rwanda [3], [19].

El Niño Southern Oscillation (ENSO)

The intensity and frequency of a two-coupled atmosphere and oceans-based tile connection, El Niño Southern Oscillation (ENSO) have been found to potentially influence the coasts of East Africa[26]. This phenomenon influences the interannual rainfall variability of Eastern Africa [27]. While the El Niño (EN) signal presents itself when the tropical sea-surface temperature (SST) in the central and eastern Pacific Ocean warmers, the southern oscillation (SO) events occur under the sign change of the east-west atmospheric pressure gradient between the tropical Pacific and Indian Oceans [28]. ENSO impacts on rainfall variability over Rwanda have been depicted by rainfall deficits for some years leading to drought as extreme weather conditions [29].

Subtropical anticyclones

High pressure- subtropical anticyclones consisting mainly of Azores, St. Helena, Mascarene, and high pressure of Arabia also influence seasonal rainfall over Rwanda. The high-pressure system of St. Helena found in the Southern Atlantic Ocean humidifies the Congo air masses and this leads to the rainfall period of March to May. The Arabian high-pressure system found in the Arabian Sea is the basis of the short dry season from December to February. Whereas the Azores' high-pressure system that is found in the Northern Atlantic Ocean improves the converges over the country, the Mascarene from the Southern Atlantic Ocean increases the humidity [30], [31]

Tropical cyclones

Also called hurricanes or typhoons or simply cyclones depending on the region, the tropical cyclones refer to the low-pressure system with a cyclonic circulation in the tropics. The tropical cyclones that significantly impact the weather to some extent over southern and eastern Africa are from the West Indian Ocean toward the Equator at twenty degrees latitude North [32].

Monsoons

East Africa and Rwanda in turn experiences rainfall influenced by the Atlantic and southeastern as well as north-eastern Indian Ocean monsoons [21], [33]. Owing to the temperature and pressure differences between land and sea, a monsoon results from a seasonal variation in the direction of the dominating winds of a given region. The dominating north-eastern Indian Ocean monsoons for the period between December and February make a transition to dominating south-eastern monsoons from June through August [34].

Easterly wave

Easterly waves of Africa or tropical waves are low-pressure wave-like oscillations characterized by a wavelength in the range from 2000km to 2500km traveling between 10 and 20º North of the tropical Atlantic and West Africa. At speeds of 7 to 8 m s^{-1} and a period of 3 to 4 days, the easterly waves vibrate from the east at an African easterly low- altitude jet [35]. African easterly waves may grow into tropical cyclones bringing about regions of cloudiness and thunderstorms (https://bit.ly/3nR6lTB).

1.6.3. Rwanda's vegetation

In Rwanda, one has two types of vegetation which are natural vegetation and artificial vegetation**.** Gishwati Forest, Mukura forest, Nyungwe forest, Birunga bamboo forest, moorland, and Akagera grasslands are examples of natural vegetation in Rwanda. Artificial vegetation is planted by humans and ranges from trees to low crops.

In 2019, Rwanda's vegetation included forests occupying 30.4% of the total country land where 53.5% were plantations,18.1% were natural mountain rainforests, 22.3% were wooded savannah and 6.1% were shrubs. Very dense forests covered 44%, moderately dense forests occupied 32%, sparse forests were 20% and 4% were much degraded. Per Province, Southern Province occupied 177,537 hectares, Western Province had 174,199 hectares of forests, Eastern province took up 274,630 hectares, Northern Province contained only 85,688 hectares and Kigali city had 12,641 hectares of forests [36].

CHAPTER TWO: LITERATURE REVIEW

2.1. Vegetation cover and its quantification

Vegetation cover, a soil portion covered by green vegetation in a given area plays too great importance in protecting the land surface and its degradation either caused by direct anthropogenic activities or climate change leads to desertification. (https://bit.ly/3C9SfQD).

Vegetation cover is a very important key factor in hydrological cycles and drives water surface water runoff, soil water yield, and controls loss of soil sediments, and thus regulates soil erosion [37]. The biodiversity in vegetation cover gives a lot of assistance directly or indirectly profitable by humanity in the ecosystem [38]. Green vegetation is reduced by the increase in urban areas [39] and this later situation enhances deforestation. Furthermore, the decrease in vegetation in the area brings about food scarcity, reduction in agricultural productivity, and poverty in turn [40]. The extent to which the vegetation is useful and the potential threats it frequently undergoes encourage different researchers to conduct studies on its degradation. For example, in its study to understand the spatial-temporal vegetation dynamics in Rwanda,[14] found about 14.1% of degradation of forest or shrubs, sparse vegetation, and grassland vegetation in Rwanda during 1990-2014. [9]found that there was a forest loss of approximately 19% from 1986 to 2006 with a peak loss from 2010 to 2014 due to public infrastructures, urban areas, and pastureland increase.[8] said that there was a decline of 65% in the natural forest between 1960 and 2007 due to the population growth. Rwanda Environment Management Authority,2021 also mentioned the like factors to be the main drivers of forest cover[41].

In several studies such as those done by [42],[43] the remote sensing resources were found to be adequate to monitor the global and regional land cover change including vegetation cover. With these resources being available, different analysis methods were used to quantify the vegetation cover change in terms of the Normalized Difference Vegetation Index (NDVI) and its climate-based causes.

2.2. Normalized Difference Vegetation Index (NDVI)

The Normalized Difference Vegetation Index (NDVI) is one of the common vegetation indices that are widely used to study the vegetation on the surface of the land[44], [45].

Being understood as the ratio of reflectance measured in two remote-sensed spectral bands, or the algebraic combination of them, the vegetation indices are of many types including the Normalized Difference Vegetation Index (NDVI), the ratio vegetation index (RVI), the green vegetation index (GVI), the leaf area index (LAI), enhanced vegetation index (EVI), to list a few [46]. The vegetation indices indicate valuable

states such as the structure of vegetation or vegetation cover, capacity in photosynthetic activity, capacity, leaf density and distribution, and water content in plant leaves. [47]. It was found to be simple and easy to use vegetation indices when one wants to get vegetation change status for the remote situation [48].

Being the standardized technique to measure healthy vegetation, the normalized difference vegetation index (NDVI) is found by dividing the difference between the near-infrared band and the red band by the sum of these two spectral bands. Generally, the green vegetation reflects less visible light and more near-infrared, less green vegetation reflects a larger part of the visible and less near-infrared. The normalized difference vegetation index has a value that is between -1 and +1. A low value of reflectance in the red band and a high value of reflectance in the near-infrared band result in a high NDVI value and the other way around. The low value of NDVI corresponds to the less or absence of vegetation(https://bit.ly/45vKtND).

Their images being normally distributed, the normalized difference vegetation index allows the elimination of topographic effects and variations in the angle of sun illumination, as well as other atmospheric elements. [44]

2.3. Climate and climate change

Climate and its change have gotten to be a prevalent theme for many writers and speakers. This may be due to the challenging effects of climate change that are imperative to be addressed. Climate is simply the statistics of weather over a longer period [49]. That is, the statistical description in terms of the mean and variability of relevant quantities over a period of at least thirty years according to the World Meteorological Organization. The germane quantities talked about here include the temperature, precipitation, and wind [50]. The climate is different from the weather in the fact that the weather refers to the short-term (over minutes to days) variations of atmospheric variables like precipitations, temperature, air pressure, cloudiness, humidity, radiations, and wind. Briefly, whereas the climate is what you expect, the weather is what you get [49]. The climate system of the Earth comprises interacting components which are the atmosphere defined as the envelope of air that surrounds the Earth, the hydrosphere consisting of liquid water on and under the earths' surface; the cryosphere which is the solid water such as sea ice, glaciers, ice sheets; and the biosphere which consists of all the living organisms.[51]

Climate change, a long-term shift in weather patterns has been found to be intensified by human activities through the burning of fossil fuels which enhances the greenhouse gas emissions in the atmosphere [52]. This increase in greenhouse gas emissions due to anthropogenic activities caused for example, the global surface temperature to be 1.1^{o}C higher during 2011–2020 than 1850–1900; the global change in observed precipitation and near-surface ocean salinity since the mid-20th century; the global mean sea level increase by 0.20 m between 1901

and 2018; the global retreat of glaciers since the 1990s and the decrease in Arctic sea ice area between 1979–1988 and 2010–2019, to list a few changes [53]. Climate change has brought about increasing weather and climate extreme events (floods, droughts, and storms) which led to acute food insecurity and lowered water security in many communities of the world and even human mortality cases pretended with 15 times higher in highly vulnerable regions, compared to regions with very low vulnerability during 2010 through 2020 [52].

2.4. Effects of climate change on vegetation cover

The climate change of the earth is bringing alterations in ecosystems even without leaving the social-economic aspects behind. The vegetation cover also is affected. The Sixth Assessment Report of the Intergovernmental Panel on Climate Change has presented that the increase by 1^{o}C of global average temperature has caused heatwaves in oceans mostly around Africa and prolonged droughts, diseases, reduction of crop productivity, range expansion of woody plants in West Africa[54].The analysis made by [55]demonstrated the vegetation influence of 52.3% by the climate change in the southern part of Gannan Prefecture, Tibetan Plateau, and 47.68% by human activities in the northern region. [56]found that there is a positive correlation between both temperature and precipitation and NDVI in Sandy land, China. In its study, [57]said that the decrease in vegetation cover due to temperature increase and droughts as well as how the land is used bring about biodiversity loss and degradation of the environment in the arid region. He predicted the coming threatening conditions of vegetation due to temperature and precipitation changes in the South Port Sudan region. Climate threats as well as man-made activities are on the basis of the decrease of vegetation cover in the Oued Lahdar Watershed, Northeastern Morocco [58]**.** Climate variables that affect NDVI vary from region to region [59]. Hussain et al (2022) showed that precipitation and temperature differently affect vegetation cover in the District Vehari of Southern Punjab (Pakistan) [60].

Like other countries of the world, Rwanda has been facing climate change risks since times ago. Among the climate change-based risks there are extreme events, including increased temperatures which lead to droughts and high rainfall leading to floods and landslides [61]. These risks are expected to affect crop production, vegetation cover, and biodiversity in Rwanda's ecosystem (https://bit.ly/3UMwdxl).Findings based on Global Circulations Models (GCMs) have shown an expected increase in temperature of up to 2 °C by the 2030s from 1970 and to 5–10 percent for average annual rainfall in the same period [1]. Alterations in the spatiotemporal distribution of vegetation bring about fluctuations in ecological and hydrological phenomena in the ecosystem[62].Rainfall and temperature changes exert a great influence on the condition of vegetation cover, one of the very important components of terrestrial ecosystems [2]. [6] got to show that there was a positive correlation of vegetation with precipitation and a moderate correlation of 40% with air temperature in Rwanda from 2000 through 2015.

It is understandable that you may need to restore vegetation cover to overcome the man-made deforestation effects but when you do not take into account climatic factors that may lead to vegetation change, ecosystem threat will remain. It is therefore of great interest to conduct research on how vegetation cover is affected by climate conditions in Rwanda as a country having a dynamic ecosystem.

2.5. Advanced Very-High-Resolution Radiometer(AVHRR) in vegetation cover monitoring

Remote sensing techniques have been mostly used in the quantification of vegetation cover through the vegetation indices that use the spectral bands sensitive to plants [48]. The most applied remote sensing satellites to monitor the vegetation cover on the land surface include the LANDSAT, AQUA, TERRA, and SPOT in their different versions and sensors, and NOOA whose sensor is AVHRR [63] from which the normalized difference vegetation index(NDVI) data sets used in this study were drawn.

Built-in the framework of the National Oceanic and Atmospheric Administration (NOAA) Climate Data Record (CDR) program, the Advanced Very High-Resolution Radiometer (AVHRR) sensor gives globally the remote sensing dataset ranging from the 1980s to recent years. This means that the Advanced Very High-Resolution Radiometer (AVHRR) is advantageous as it embeds the accessible important data source that may be used when one wants to do a study of long-term changes in properties of the land surface because it generates the longest time-series of global satellite records [64]. The Advanced Very High-Resolution Radiometer (AVHRR) has also the advantage of providing a dataset in temporal resolution of daily global coverage.

Launched in 1981, the AVHRR sensors have had four channels that sensed data in the visible red, near-infrared, shortwave-infrared, and thermal channels. Two channels of Advanced Very High Resolution Radiometer (AVHRR), one with wavelength ranging from 0.58 to 0.68 μm which is sensitive to red reflected light and another whose wavelength ranges from 0.725 to 1.10μm sensitive to infra-red reflected light have been in most wide use in differentiating and checking the vegetation condition [65].

2.6. MPI-REMO model

Generally, one may refer to a climate model to a mathematical representation of the climate system based on physical and biological as well as chemical principles. Regional climate models present the similarity to a global climate model in the fact that both provide the simulation of the physical processes in the climate system. However, the simple difference is that regional climate models enclose the limited space of the globe and then run at much smaller spatial resolution from 1 to 50 km grid spacing whereas the global climate model may be run at spatial resolution form 100-300 km grid spacing. It is in that case that the regional climate models can simulate large-scale weather patterns and the local terrain interactions [51].Driven by the Global

climate models (GCMs), the regional models (REMO) have been used in different world regions including Africa domain and it has been found to be suitable for long-term climate change modeling so that to understand the projected future changes in all the regions [66].

MPI-REMO is one of the Regional Climate Models (RCM) driven by Max Planck Institute for Meteorology's Earth System Model at low resolution (MPI-ESM-LR) as a Global Climate Model (GCM) and it was made at Climate Service Center (CSC) in Hamburg, Germany[67]. MPI- REMO has a spatial horizontal resolution of 50km and temporal simulation which is between 1951 and 2100 [68].On a global basis, the simulations are downscaled with REMO over the Coordinated Regional Climate Downscaling Experiment (CORDEX) [69] which is online available on the Earth System Grid Federation (ESGF) portal. MPI-REMO has been used in simulating the mean temperature and precipitation in different parts of Africa [70].

2.7. Representative concentration pathways.

Different technologies have haven put in place to predict the contribution of the amount of greenhouse gases that will be emitted to future global warming to enhance climate change. Among the means that are used, there are the scenarios that include the Representative Concentration Pathways (RCPs). A scenario is defined as the plausible trajectory of different aspects of the future that is constructed to investigate the potential consequences of anthropogenic climate change (https://bit.ly/3CfBXJc).

Available Representative Concentration pathways (RCPs**)** are RCP 8.5 which is a high pathway for which radiative forcing reaches more than 8.5 watts per meter squared (approximately 1370 ppm CO_2 eq) by 2100 and continue to rise for some amount of time; RCP 6 which is the pathway for which radiative forcing is stabilized at approximately 6watts per meter squared (approximately 850 ppm CO_2 eq) after 2100; RCP 4.5 which is the pathway for which radiative forcing is stabilized at approximately 4.5 watts per meter squared (approximately 650 ppm CO_2 eq) after 2100; and RCP 2.6 which is the pathway for which radiative forcing peaks at approximately 3 watts per meter squared (approximately 490 ppm CO_2 eq) before 2100 and then shows the decline [71].The Representative concentration pathways (RCPs**)** are widely applied to serve as input to Climate models; they ease pattern scaling of climate model outputs, they are used in the exploration of the range of socioeconomic conditions that are consistent with a given concentration pathway and they may be used to explore the climate implications of spatial forcing patterns [72].

CHAPTER THREE: DATA AND METHODOLOGY

3.1. Sources and description of data

3.1.1. The historical climate station-recorded data

In this study**,** rainfall and temperature data sets have been used. They are, in fact, the most common climate variables that demonstrate considerably the change of climate and affect the vegetation cover. Enhancing National Climate Services (ENACTS) data of rainfall and temperature recorded on a daily basis over Rwanda between 1983 and 2020 were collected from the Rwanda Meteorological Agency. ENACTS data have been useful to get rid of the gaps in the station observations [73]. The spatial locations of selected stations are given in the **table1.**

3.1.2. Historical NDVI remote sensing datasets

We have quantified the vegetation cover by means of the Normalized Difference Vegetation Index (NDVI). Even if there are many vegetation indices, the Normalized Difference Vegetation Index is the most commonly used parameter to understand the vegetation density as well as the variations in plant health in a given area over time. Recently, the NDVI has been largely used to determine the inter- relationship between vegetation dynamics and climatic variables [4].In addition, NDVI quantifies the vegetation cover and its change [74].

NDVI remote sensing data over the 1983-2020 period have been online downloaded from the Advanced Very-High-Resolution Radiometer (AVHRR) sensor onboard the National Oceanic and Atmospheric Administration version 7 (NOAA-7) Climate Data Record (CDR) satellite (https://bit.ly/3VGWs7i). The Advanced Very-High-Resolution Radiometer (AVHRR) sensor provides daily gridded Normalized Difference Vegetation Index (NDVI) with spatial resolution of 0.05x0.05 degrees (~5.5km) calculated globally over land surface reflectance. The Normalized Difference Vegetation Index (NDVI) data encompassed by NOAA-CDR satellite have so good quality standards that they ensure consistency and reliability in using them. (https://bit.ly/3VJmK8M)

The Normalized Difference Vegetation Index (NDVI) was calculated from the red band (RED) and near – infrared (NIR) band [75]. The following formula is used to compute the value of NDVI:

$$\mathrm{NDVI} = \frac{\mathrm{NIR} - \mathrm{RED}}{\mathrm{NIR} + \mathrm{RED}} \quad (1)$$

For our case of NOAA/AVHRR images, the red band is represented by Band 1 (580-680nm), and the near-infrared band is represented by Band 2 (725-1100nm) [45]. That is,

$$NDVI = \frac{C2 - C\ 1}{C2 + C1} \quad (2)$$

where C_1 and C_2 stand for Band 1 and Band 2 respectively.

The Normalized Difference Vegetation Index varies between -1 and +1. The types of vegetation and the corresponding threshold range of NDVI values are in **Table 2***(https://bit.ly/3VI0A6Y)*, [76].

3.1.3. The projected climate datasets

Projected rainfall and temperature datasets over Rwanda were downscaled on a daily scale by the regional climate model, MPI-REMO. MPI-REMO is one of the Regional Climate Models (RCM) from the Coordinated Regional Downscaling Experiment (CORDEX) project and is driven by a Global Climate Model (GCM)of MPI-ESM-LR and was made at Climate System Center (CSC) in Hamburg. MPI-REMO model has a spatial resolution of $0.5^0 \times 0.5^0$ (approximately 50km x 50km) and was ranked to be among the best performing regional climate models for precipitation and/or temperature and then advised to utilize it for more analysis of future climate over Rwanda [77], [78].

3.2. Methodology

3.2.1 Rainfall and temperature analysis

Both rainfall and temperature as climate variables have been analyzed to show how they varied from 1983 to 2020 in Rwanda.

3.2.1.1. Annual spatial-temporal variation of rainfall and temperature

Annual spatial-temporal variability of rainfall and temperature have been analyzed to show the annual rainfall and temperature climatology from 1983 to 2020 for historical situations and from 2024 to 2053 for future prediction.

3.2.2. Normalized Difference Vegetation Index (NDVI) analysis

The Normalized Difference Vegetation Index (NDVI) data have been downloaded in netcdf format on a global map basis and extracted using Climate Data Operator(CDO) to obtain the NDVI map for Rwanda and then the Climate Data Tool(CDT) was used to get NDVI values in excel format.

3.2.2.1. Annual and spatial-temporal variation of NDVI

The annual variation of NDVI during the 1983 to 2020 period in Rwanda has been analyzed. The trends of NDVI gave insight into how it has changed during the thirty-eight years.

3.2.3. Statistical analysis

The subjectivity of the perceptual method of trend is so not enough that statistical analysis is required for deep understanding. Statistical methods have been used in different studies to analyze climate data [79], [80].

3.2.3.1. Mann-Kendall test for trend direction.

In this study, the trends in the time series of NDVI and climate variables were tested statistically using the Mann-Kendal (MK)test to analyze their significance at the confidence level of 95%.

Mann-Kendal test has been used to determine the type of direction of the trends of temperature, rainfall, and NDVI during the periods chosen. It is a non-parametric method that has been widely used in time series data to test the kind of their trends [81]–[83] with the advantages of less influence of outliers and other forms of normality. The statistics of Mann-Kendall are the following:

$$S = \sum_{i=1}^{n-1} \sum_{j=i+1}^{n} \text{sign}(V_j - V_i) \tag{3}$$

Where n is the number of time series values; V_i and V_j are annual values in years i and j with j>i, and the sign function $sign(V_j - V_i)$ is given by:

$$\text{sign}(V_j - V_i) = \begin{cases} -1 \text{ for } (V_j - V_i) < 0 \\ 0 \text{ for } (V_j - V_i) = 0 \\ +1 \text{ for } (V_j - V_i) > 0 \end{cases} \tag{4}$$

The variance of S was determined using the following equation:

$$\sigma_S = \frac{n(n-1)(2n+5) - \sum_{i=1}^{m} w_m(w_m - 1)(2w_m + 5)}{18} \tag{5}$$

Where σ_S is the variance of S; n is the number of data points, and m is m is the number of tied groups and $w_m$stands for the number of ties in mth group. A tied group refers to the same value sample in the dataset.

The standard normal test statistic T_S was calculated to verify if there exists a statistically significant trend and the following equation was used:

$$T_S = \begin{cases} \frac{S-1}{\sqrt{\sigma_S}} \text{ for } S > 0 \\ 0 \quad \text{for } S = 0 \\ \frac{S+1}{\sqrt{\sigma_S}} \text{ for } S < 0 \end{cases} \tag{6}$$

If $T_S > 0$, one has an increasing or upward trend whereas if $T_S < 0$, the decreasing or downward trend presents itself. At a significant level β one rejects the null hypothesis H_0 if $|T_S| > T_{S_{1-\beta/2}}$ where $T_{S_{1-\beta/2}}$is drawn from the standard normal distribution tables. In this study, β was taken to be 0.05.

3.2.3.2. Sen's slope estimator for quantification of trends.

Sen's slope goes with the Mann-Kendall test. Sen's Slope estimator is furthersome in the fact that it is not influenced by outliers and errors in datasets [84].

$$\mu = \text{median}\frac{(V_j - V_i)}{j - i}, j > i \tag{7}$$

Where μ is the Sen's slope estimator; V_i is the annual value of temperature/precipitation/NDVI at year i; V_j is the annual value of temperature/precipitation/NDVI at year j.

This formula implies that:

$$\mu = \begin{cases} \mu_{\frac{N+1}{2}}, & \text{if N is odd} \\ \frac{1}{2}\left(\mu_{\frac{N}{2}} + \mu_{\frac{N+2}{2}}\right), & \text{if N is even} \end{cases} \tag{8}$$

Where N are the values of slopes of all data value pairs in the datasets.

For $\mu > 0$, one has a positive trend, and when $\mu < 0$ the trend is negative.

The version of the prewhitened Mann-Kendall was used because it gives the results after removing the serial autocorrelation present in the datasets[85].

3.2.3.3. Coefficient of variation

In this study, the coefficient of variation (CV) has been analyzed to evaluate the variability of temperature, rainfall, and Normalized Difference Vegetation Index(NDVI) at an annual scale. The coefficient of variation is defined as the measure of the extent to which the data points disperse from the mean in a set of data series. Expressed in percentage, it is quantitatively given by the ratio of the standard deviation to the mean of the data set.

$$C.V = \frac{\delta}{\bar{X}} \times 100 \tag{9}$$

where δ is the standard deviation and $\bar{X}$ is the mean. The greater the coefficient of variation, the larger the variability of the considered variable.When CV<10%, 10% < CV <20%, 20% < CV <30%, or CV>30% the coefficient of variation, consequently the variability is low, medium, high, or very high respectively[86].

3.2.3.4. Correlation and linear regression analysis

The statistical linear regression method helped to determine the relationship between NDVI and both temperature and rainfall over the study region. The Pearson correlation coefficient has been calculated as:

$$r = \frac{n(\sum XY) - \sum X \sum Y}{\sqrt{\left[n\sum X^2 - (\sum X)^2\right] - \left[n\sum Y^2 - (\sum Y)^2\right]}} \tag{10}$$

Here, r is the Pearson correlation coefficient; X is the independent variable (rainfall or temperature); Y is the dependent variable (NDVI) and n is the number of data sets.

The Pearson correlation coefficient varies between +1 and -1. If the Pearson correlation is +1, one has a perfect positive correlation and a perfect negative correlation when it is equal to -1. The Pearson correlation which is equal to 0 implies no correlation between variables [54]. Other threshold ranges of the Pearson correlation coefficient and their implications are in **Table 3**.[76], [87].

3.2.3.5. Multilinear regression analysis

The multilinear regression method was used to relate the Normalized Difference Vegetation Index and both temperature and rainfall. This method has been found to be useful in assessing the relationships between variables [88]. The equation for this statistical technique was formulated as follows:

$$\mathrm{NDVI} = \alpha_0 + \alpha_1 \mathrm{R} + \alpha_2 \mathrm{T}_{\mathrm{mean}} \quad (10)$$

Where $NDVI$ is the Normalized Difference Vegetation Index; T_{mean}, R are annual mean temperature and rainfall at any time period considered respectively; $\alpha_0, \alpha_1, \alpha_2$, are coefficients that have been determined from historical data (from 1983 to 2020).

3.3. Prediction of NDVI

Vegetation cover in different regions of Rwanda has been predicted being represented by the Normalized Difference Vegetation Index (NDVI). The projected rainfall and temperature of the future period of 2024 to 2053 were found via the MPI-REMO model explained in section 3.1.3 above. After making a bias correction using the template of Linear Scaling Bias Correction version 1.0, MPI-REMO model-based data of rainfall and temperature were put in the multilinear equation 10 above to get the data of NDVI from 2024 through 2053. The future NDVI data were represented in the same process as for the historical data visualization.

Plotting tools

The Geographic Information System (GIS) version 10.8 through the process of ordinary kriging was used to visualize the spatial distributions of variables and coefficients in consideration on the maps. The ordinary kriging interpolation is widely used in interpolation of precipitation and temperature [89], [90]. Excel software was used to plot the temporal variations of different variables and coefficients. We note that all tables and figures have been put in the addendum section.

CHAPTER FOUR: RESULTS AND DISCUSSION

Chapter four embeds the analysis and discussion of the results obtained after carrying out the methods in the methodology scheme.

4.1. Spatial distribution of average annual rainfall, average annual mean temperature, and average NDVI in Rwanda from 1983 to 2020.

4.1.1. Spatial distribution of average annual rainfall in Rwanda from 1983 to 2020.

The spatial distribution of average annual rainfall in Rwanda from 1983 to 2020 has been mapped and shown in **Figure 4a.** The overall average annual rainfall in the study area was 1239mm and the map reveals that the highest annual rainfall (between 1890 and 2018mm) was at West-East of Western Province for example at Cyato whereas the lowest annual rainfall (between 853 and 983 mm) was at and near Rwimbogo, Kawangire, and Mpanga in the Eastern Province. The central plateau had the annual rainfall ranging from 1113 to 1242mm. Generally, the Eastern Province, the East region of Southern Province, and Kigali City presented themselves as having lower rainfall than other provinces. This coincides with the findings in [16].

4.1.2. Spatial distribution of average annual mean temperature in Rwanda from 1983 to 2020

The spatial distribution of the annual average maximum temperature in Rwanda from 1983 to 2020 has been mapped and shown in **Figure 4b.** The overall average annual mean temperature in the study area was 19.82^{o}C and the map reveals that the highest mean temperature (between 22.65 and 23.44^{o}c) was at and near Bugarama in the Western Province whereas the lowest mean temperature (between 16.18 and 16.99^{o}C) was at and near Ruhengeri and Kinoni in the Northern Provinces. Eastern Province felt in the range of mean temperature between 20.23 and 21.2^{o}C except at Nyamata, Rwimbogo, and Karangazi where the mean temperature was between 21.3 and 21.83^{o}C. The South –West of the Western Province showed the highest ranges of mean temperatures whereas the Northern Province was the coldest.

4.1.3. Spatial distribution of average annual NDVI in Rwanda from 1983 to 2020

The spatial distribution of the annual average normalized difference vegetation index (NDVI) in Rwanda from 1983 to 2020 has been mapped and shown in **Figure 4c**. The map reveals that in general, the study area felt in two ranges of low NDVI($0<NDVI<0.1$) and moderate NDVI($0.2<NDVI<0.5$), the great part of the South Province, the south-west past of Eastern Province and at and near Rubengera in the Western Province have the largest values of NDVI between 0.22 and 0.23. The lowest values of low NDVI (between 0.14 and 0.16) were located mainly in the Northern Province at Ruhengeri, Kinoni, and Gisenyi and at Cyato in the

Western Province. The NDVI map also tells us that there were no regions in consideration with non-vegetation because NDVI values are all greater than 0 but the sparse vegetation that is, grasslands and shrubs dominated.

4.2. Temporal variations of average annual rainfall, average annual mean temperature, and average annual NDVI in Rwanda from 1983 to 2020.

4.2.1. Temporal variations of annual mean rainfall in Rwanda from 1983 to 2020.

The temporal variation of annual mean rainfall in Rwanda from 1983 to 2020 has been assessed and the results are shown in **Figure 5(i)**. The trend shows that the rainfall increased from 1983 to 2020 with a slope of $0.7\text{mm}year^{-1}$where it reached the highest values of 1631mm in 1997 and 1589mm in 2003mm respectively and the lowest values of 913mm in 1984 and 556mm in 2017 respectively.

4.2.2. Temporal variations of average annual mean temperature in Rwanda from 1983 to 2020.

The temporal variation of average annual mean temperature from 1983 to 2020 has been assessed and the results are shown in **Figure 5(ii)**. The trend shows that the mean temperature was changed from 1983 to 2020 by approximately 0.2ºC and the highest values of 20.22, 20.24,20.54, and 20.55ºC were reached in 1998, 2005,2016 and 2020 respectively. The lowest values of 19.18, 19.19,19.17, and 19.21 ºC were observed in 1986, 1985, 2011, and 2001 respectively.

4.2.3. Temporal variations of average annual NDVI in Rwanda from 1983 to 2020.

The temporal variation of average annual NDVI from 1983 to 2020 has been assessed and the results are shown in **Figure 5(iii)**. The trend shows that the mean temperature increased from 1983 to 2020 with the slope of approximately $0.0007year^{-1}$ where the maximum value was 0.23 in 2016 and the minimum value of 0.16 in 1988.

4.3. Coefficient of variation analysis

4.3.1. Spatial annual coefficient of variation of rainfall, mean temperature, and NDVI

At the annual time scale, the spatial coefficient of variation(cv) of average annual rainfall, mean temperature, and average annual NDVI in Rwanda from 1983 to 2020 has been represented in the maps of **Figure 6**. All regions in the study area felt in high variability in rainfall (20%<cv<30%), the Eastern Province and Kigali City being in the largest range (between 25.9 and 27.3%). The smallest range of variability in rainfall (between 21.3 and 23%) was in the Western Province at Murunda and Rubengera and the Northern Province at Ruhengeri **(Fig 6. A).** The variability of mean temperature was low (cv<10%) and unequally distributed in the study area, with the Northern Province at Kinoni having the largest range (between 3.4 and 3.8%). The

Eastern Province and the Western Province at Bugarama and Murundi experienced the smallest range of variability (between 1.8 and 2.3%) **(Fig 6. B).** There was a medium variation of NDVI in the study area from 1983 to 2023 with unequal distribution. The largest range of coefficient of variation (between 14 and 14.8%) was in the southwest part of Eastern Province, especially at Bugarama. The smallest coefficient of variation was in the Eastern Province with values between 11.2 and 12.1% **(Fig 6. C)**

4.3.2. Temporal annual coefficient of variation of average annual rainfall, annual mean temperature, and average annual NDVI in Rwanda from 1983 to 2020

The temporal coefficients of variation of average annual rainfall, annual mean temperature, and annual average NDVI are shown in **Figure 7.** It is clear that rainfall showed a medium variability in 2003 and 2020 (10<CV<20%), very high variability in 1984, 1988,1991-1993, 2005,2008-2010, and 2012-2017(CV>30%), and other years where characterized by high variability in rainfall (20<CV<30%). The considerable fluctuations in rainfall during these years might be caused by El Niño Southern Oscillations years which have taken since the 1960's in differents parts of Rwanda [91]. For mean temperature, the variability was in the medium range from 1983 to 2014 and low from 2015 to 2020. The NDVI had low variability in 2000, and high in 2015, 2016, 2019, and 2020. Other years where characterized by medium variability in NDVI.

4.4. Mann-Kendall Test analysis of average annual rainfall, annual mean temperature, and average annual NDVI in Rwanda from 1983 to 2020

To test the existence and significance of trends for mean temperature, rainfall, and Normalized Difference Vegetation Index (NDVI) at an annual scale; the analysis was done at a 95% significance level by means of Mann-Kendall test statistics and the estimator of Sen's slope. The results found are summarized in **Table 4** including the Mann-Kendal standardized test statistics (T_s) to show the direction of the trend, the Sen's slope(μ) to quantify the magnitude of the trend, p-value for the significance evaluation of the trend at a 95% significance level.The symbol (*) in the tables means that the trend is significant and the empty space implies a non-significant trend. The results communicate that the trends existed ($T_s \neq 0$)at all stations for mean temperature from 1983 to 2020 except at Rubengera (T_s=0) and that significant increasing trends (T_s> 0, P-value <0.05) were at Kanombe, Gikonko, Butare, Musambira, Kabgayi, Busasamana, Byumba, Ruhengeri, Kivumu, Cyato, Rwimbogo, Nyamata, and Kibungo at respective slopes of $0.012℃year^{-1}$, $0.016℃year^{-1}$, $0.012℃year^{-1}$, $0.014℃year^{-1}$, $0.015℃year^{-1}$, $0.018year^{-1}$, $0.010℃year^{-1}$, $0.011℃year^{-1}$, $0.015℃year^{-1}$, $0.013℃year$, $0.011℃year^{-1}$, and $0.012℃year^{-1}$and there was no decreasing trend (T_s< 0) for the annual mean temperature at any station.

Concerning the rainfall, the increasing trend was at Rwimbogo with a slope of $6.230mmyear^{-1}$ whereas others considered regions presented non-significant trends at a 95% confidence level. The NDVI on its hand showed decreasing significant trends (T_s< 0, P-value <0.05) at Gitega, Cyato at the same rate of $-0.0006year^{-1}$ although the

increasing significant trend was at Butare, Gikonko, Musambira, Kabgayi, Busasamana, Muganza, Byimana, Gisenyi, Bugarama, and Karangazi with slopes of $0.0060 year^{-1}$, $0.0085 year^{-1}$, $0.0084 year^{-1}$, $0.0079 year^{-1}$, $0.0099 year^{-1}$, $0.0058 year^{-1}$, $0.0271 year^{-1}$, $0.0001 year^{-1}$, $0.0100 year^{-1}$, and $0.0271 year^{-1}$ respectively.

4.5. Relationship between the Normalized Difference Vegetation Index (NDVI) and average annual rainfall and annual mean temperature

Both the spatial and temporal correlation existing between NDVI and annual rainfall or mean temperature have been shown based on the coefficient of correlation (r). The results are given in **Table 5**. The output table revealed that the spatial coefficient of correlation between the normalized difference vegetation index (NDVI) and the average annual rainfall or mean temperature depends on the region in the study area. This is reasonable because the mean temperature and the rainfall are not quantitatively the same in all areas with time.

The map shows that the correlation between NDVI and rainfall or temperature is not uniform in the study area. Whether positively or negatively, the correlation of NDVI to average annual rainfall was unequally very low in general with a positive low correlation between 0.14 and 0.17 at Muganza, Butare, Gikonko, and Nyamagabe in the Southern Province for instance (**Figure 8.1**). The correlation of NDVI to mean temperature was also unequally distributed in the study area. However, the NDVI was more correlated to mean temperature than rainfall in different regions of the study area. For example, at Muganza, Butare, Gikonko, and Nyamagabe in the Southern Province where there was a very low correlation with the rainfall, one had a medium correlation with mean temperature. At Ruhengeri and Kinoni in the Northern Province where the correlation was very low with the rainfall, it was moderate with mean temperature (**Figure 8.2**).

The temporal coefficient of correlation between NDVI and annual mean temperature as well as average annual rainfall was shown in the graph represented in **Figure 9**. The NDVI was positively correlated to mean temperature and either positively or negatively to average annual rainfall during the 1983-2020 period. The temporal coefficient of correlation between NDVI and either average annual rainfall or annual mean temperature varies from year to year during the considered period. This may be caused by the fact that the considered variables do not show the same averaged values in different years.

4.6. Results from multilinear regression

Multilinear regression has been used to evaluate the relationship between NDVI and both average annual rainfall and annual mean temperature from 1983 to 2020. The equation has been computed using Excel software and the formula has been found to be:

$$\mathrm{NDVI} = -0.3 + 0.00002\mathrm{R} + 0.02\mathrm{T}_{\mathrm{mean}} \qquad (12)$$

Where NDVI is the Normalized Difference Vegetation Index; R is the average annual rainfall; T_{mean} is the average annual mean temperature.

4.7. Prediction in the future

In this work, the predicted NDVI was performed through the MPI- REMO model with the basis of two selected Representative Concentration Pathways: RCP 2.6 and RCP 8.5 outputs whose bias correction was done using observed meteorology stations data and the historical data of the model. The coefficients in the equation of multilinear regression relating the NDVI and both rainfall and mean temperature were computed based on the observed data recorded on 29 meteo stations. This equation was used to get the predicted data of NDVI from 2024 to 2053 where R and T_{mean} taken at this stage are the rainfall and mean temperature under RCP 2.6 or RCP 8.5.

4.7.1. Spatial distribution of predicted average annual rainfall, annual mean temperature, and NDVI under RCP 2.6 and RCP 8.5

The spatial distribution of predicted average annual rainfall under RCP 2.6 and RCP 8.5 during 2024-2053 has been represented in **Figure 10 (i)** and **Figure 11 (i)** respectively**.** The map in figure 10 (i) shows that the minimum average annual rainfall will be between 538 and 1061 mm in a great part of the Eastern Province at Rwimbogo, Kawangire, Mpanga, and Karangazi; at Gisenyi of the Western Province even at Ruhengeri and Byumba in the Northern Province. Considerable maximum average annual rainfall will be concentrated in the south-west of the Southern Province especially at Muganza (2629-3151mm) and the south region of the Western Province at Bugarama (2017-2628 mm). In general, the rainfall will increase from the Eastern Province to the Central Plateau and then to the Western Province. The map in **Figure 11(i)** shows that the minimum average annual rainfall will be between 509 and 1021 mm in a great part of the Eastern Province at Rwimbogo, Kawangire, Mpanga, Karangazi, and Mwurire even at Ruhengeri in the Northern Province. Considerable maximum annual average rainfall(2558-3069mm) will be at Byimana in the Southern Province. The maps show that the average annual rainfall under high emission will be of lower intensity than under low emission in different parts of Rwanda.

The spatial distribution of predicted average annual mean temperature under RCP 2.6 during 2024-2053 has been represented in **Figure 10(ii)** and **Figure 11(ii)** respectively. The lower mean temperature (18-19^{o}C) will be in the Northern Province, especially at Ruhengeri and Kinoni. The higher mean temperature (23^{o}C) will be at Bugarama in the Western province. The great part of Eastern Province, Kigali City, and the south region of Southern Province will present a high temperature of 22^{o}C. In general, the mean temperature will increase from south to north in each Province (**Figure 10 (ii**)). Under RCP 8.5, temperature (18-19^{o}C) will be in the

Northern Province especially at Ruhengeri and Kinoni, at Gisenyi in the Western Province, and Kibungo in the Eastern province. The higher mean temperature of 24^{o}C will be at Bugarama in the Western province. The average annual mean temperature will be greater under RCP 8.5 than under RCP 2.6 in most parts of the study area. This implies that to control the temperature quantity in an area, one should take into account the emissions in the atmosphere.

The spatial distribution of the predicted average annual Normalized Difference Vegetation Index (NDVI) under RCP 2.6 and RCP 8.5 during 2024-2053 has been represented in **Figure 10(iii)** and in **figure 11(iii)** respectively. In consideration of the two scenarios, the land will be covered with vegetation. The low values of NDVI will be dominant at Kinoni, Gisenyi, and Ruhengeri under RCP 2.6 and RCP 8.5 whereas the moderate values of NDVI will be at Bugarama in the Western province. The NDVI will increase from the north to south and from East to west of the study area under the scenarios.

4.7.2. Temporal variability of NDVI during 2024-2053 under RCP2.6 and RCP 8.5

The variability of the average annual normalized difference vegetation index(NDVI) from 2024 to 2053 for the two scenarios RCP2.6 and RCP 8.5 were plotted in **Figure 12**. The trends show the increase of the NDVI values with a slope of $0.0009 year^{-1}$ and $0.0002 year^{-1}$ at the high emission and low emission respectively. The highest low-range NDVI value of 0.16 will be in 2043 and 2053 for RCP 8.5 and the value of 0.17 in 2044 for RCP 2.6

4.7.3. Temporal coefficient of variation of predicted average annual rainfall, annual mean temperature, and average annual NDVI.

The coefficients of variation of predicted average annual rainfall, annual mean temperature, and average annual NDVI under RCP 2.6 and RCP 8.5 have been plotted in **Figure 13.** The highest coefficient of variability in average annual rainfall will be approximatively 60% in 2043 for RCP 2.6 and 57% in 2035 for RCP 8.5. The lowest coefficient of variation in average annual rainfall will be approximatively 39% in 2052 for RCP 2.6 and 32% in 2033 for RCP 8.5. In general, the variability of rainfall will not be uniform through the period of 2024-2053 for the two scenarios (**figure 13(b))**. The coefficient of variation for the average annual mean temperature will be approximately 14% and 11% respectively under RCP 8.5 and RCP 2.6 throughout the period of 2024-2053. The variability in mean temperature will be approximately uniform throughout the considered period under the two scenarios (**figure 13(c))**. The NDVI coefficient of variation will be between 27 and 38% for RCP2.6 and between 38 and 49% under RCP 8.5. The variability in NDVI under RCP 2.6 is smaller than under RCP 8.5 (**figure 13(a))**. This stresses that the emission of greenhouse gases in the atmosphere generates considerable variation in vegetation cover. Low emission brings about small changes in vegetation cover while high emission causes large changes in vegetation cover.

4.7.4. Spatial coefficient of variation of Predicted average annual rainfall, average annual mean temperature, and average annual NDVI.

Spatially, many regions in the study area fall in high-range of coefficient of variation in predicted average annual rainfall under RCP 2.6 where the highest coefficient of variation (27-29%) will be at Ruhengeri and Bigogwe in Northern Province. The smallest medium-range (13-16%) of coefficient of variation will be in the south –west of the Southern Province and the south region of the Western Province (**Figure 14. A).** Under high emission, the medium-range variation (10<CV<20%) in predicted average annual rainfall will be concentrated in the great part of the Northern Province where the smallest values in coefficient of variation will be between 17.1% and 19.1%. The large part of the study area will have a coefficient of variation between 19.2% and 20.1%. The high-range variation (20<CV<30%) will dominate the south part of the Southern Province and Western Province (**Figure 15. A**)

As long as the predicted average annual mean temperature is concerned under RCP 2.6, it will show non-uniformly low variation (CV<10%) in the study area where large variation tends to be in Southern Province, Western Province and (2.7<CV<3 %) (**Figure 14. B**). Under high emissions, the predicted average annual mean temperature will fall in non-uniform low-range variation (CV<10%) (**Figure 15. B).** However, the two maps show that high emissions will bring about larger variability in annual mean temperature than at low emissions during 2024-2053.

The predicted annual average NDVI on its hand under RCP 2.6, will also fall in the low-range variation where the largest values will be at Kinoni and Ruhengeri in Northern Province. The lowest variation will be in the southern regions of the Southern Province, Western Province, Kigali City, and a great part of Eastern Province (**Figure 14. C).** Under high emissions, a great part of the study area will fall in low-range variation in the predicted annual average NDVI where the lowest variation will dominate the south region of the Eastern Province especially at and near Mwurire and Kibungo. The largest medium-range variation (between 15 and 19%) will be in the northwest of the western Province, especially at Bigowe, Gisenyi, and Murunda, northwest of Northern Province at and near Kinoni **(Figure 15. C).** In general**,** the variability in NDVI will fluctuate from region to region in the study area under the considered emission.

4.7. 5. Spatial coefficient of correlation of predicted average annual rainfall, average annual mean temperature, and average annual NDVI under RCP 2.6 and RCP 8.5.

The relationship between predicted average annual NDVI and both average annual rainfall and average annual mean temperature is represented in **Figure 16.** The diagram tells us that under RCP 2.6 and RCP8.5, the NDVI will either negatively or positively be correlated to rainfall with non-uniform low correlation from region to region (**Figure 16. a1 and 16. b1**). It will be correlated positively to mean temperature with a high

correlation(0.6<r<0.79) at Buganza and Cyato and with a very high correlation (0.8<r<0.9) at other regions under RCP 2.6 (**Figure 16. a2)**. Under RCP 8.5, the predicted average annual NDVI will be correlated positively to mean temperature with non-uniform very high correlation(0.8<r<0.9) from region to region in the study area (**Figure 16. b2)**. It is shown that general the average annual NDVI will be more correlated to annual mean temperature than annual rainfall under the two scenarios in consideration.

4.8. Man-Kendall statistics of predicted average annual NDVI, average annual rainfall, and average mean temperature under RCP 2.6 and RCP 8.5

Man-Kendall statistics of predicted average annual NDVI, average annual rainfall, and average annual mean temperature under RCP 2.6 and RCP 8.5 were summarized in **Table 6, Table 7,** and **Table 8 r**espectively. Table 6 reveals that there will be the existence of the trends of NDVI under the two scenarios at all stations in consideration. However, at a significance level of 95%, the trends will be insignificantly increasing except at Cyato where there will be an insignificantly decreasing trend at the slope of $2.4E-05\ year^{-1}$ under RCP 2.6. Under high emission (RCP 8.5), one will have significant increasing trends except at Musambira, Gikongoro, Muganza (Southern Province), Cyinzuzi, Kinoni (Northern Province), and Murunda (Western Province) where the trends will be insignificantly increasing.

Similarly, the rainfall trends will exist under the two selected scenarios at all considered stations. However, at the significance level of 95%, trends will be insignificantly increasing except at Karangazi where there will be a significantly increasing trend at a slope of $6.9739\ \text{year}^{-1}$ under RCP 2.6. Under high emission (RCP 8.5), one will have insignificant decreasing trends except at Cyinzuzi, Byumba, and Bigogwe where the trends will be significantly decreasing at slopes of $-9.2598\ \text{year}^{-1}, 9.2598\ \text{year}^{-1}, -7.0643\ \text{year}^{-1}, -7.3823\ year^{-1}$ respectively (**Table 7**).

The mean temperature will present trends at all stations under the two scenarios at all selected stations. However, at the significance level of 95%, trends will be insignificantly increasing except at Masaka where there will be an insignificantly decreasing trend at the slope of $-0.0013 year^{-1}$ under RCP 2.6. Under high emission (RCP 8.5), one will have significant increasing trends except at Gitega, Kanombe, Byumba, Mpanga, Kawangire, and Kibungo where the trends will be insignificantly increasing **(Table 8).**

CHAPTER FIVE: CONCLUSION AND RECOMMENDATIONS

This study aimed at the prediction of future vegetation cover in response to climate change in Rwanda. The vegetation cover has been monitored through the normalized difference vegetation Index (NDVI) whereas the temperature and precipitation (rainfall) were considered as the climate factors to be related to the normalized difference vegetation index. The rainfall, temperature, and NDVI during 1983-2020 for the historical annual variability and during 2024-2053 for future prediction have been analyzed. The coefficient of variation was used to quantify the variability and the Person correlation coefficient helped to show the degree of relationship between the Normalized Difference Vegetation Index and both rainfall and temperature. MPI-REMO model on the basis of two Representative Concentration Pathways: RCP 2.6 and RCP 8.5 was used to get future data for prediction and the statistical Mann-Kendall test was used to analyze the existence of the trends of NDVI and climate factors in consideration where the significance level was evaluated at 95%.

The spatial distribution revealed that the Eastern Province, the East region of Southern Province, and Kigali City presented themselves as having lower rainfall than other provinces from 1983 to 2020 The rainfall will increase from Eastern Province to the Central Plateau and then to the Western Province from 2024 to 2053 under RCP 2.6. and generally, the average annual rainfall under high emission will be of lower intensity than under low emission in different parts of Rwanda. The southwest of the Western Province showed the highest ranges of mean temperatures whereas the Northern Province was the coldest Province from 1983 to 2020 and it will increase from south to north in each Province from 2024 to 2053 under RCP 2.6. Generally, the average annual mean temperature will be greater under RCP 8.5 than under RCP 2.6 in the most part of the study area. The grasslands as well as the shrubs dominated many regions in the study area as the ranges of the NDVI implied from 1983 to 2020 and NDVI will increase from the North to South and from East to West of the study area under the scenarios in consideration from 2024-2053.

On the temporal scale, the rainfall increased from 1983 to 2020 with a slope of 0.7mm$year^{-1}$where the highest value of 1631mm was in 1997 and the lowest value of 556mm was in 2017. The mean temperature changed by approximately 0.2^{o}C where the highest value of 20.55^{o}C was reached in 2020 and the lowest value of 19.18^{o}C were observed in 1986. The NDVI increased at a rate of approximately 0.0007 year^{-1} where the maximum value of 0.23 was in 2016 and the minimum value of 0.16 was in 1988.
The NDVI will increase with the slope of 0.0009$year^{-1}$ and 0.0002$year^{-1}$ at the high emission and low emission respectively. The highest low-range NDVI value of 0.16 will be in 2043 and 2053 for RCP 8.5 and the value of 0.17 in 2044 for RCP 2.6.

During 1983-2020, all regions in the study area experienced high variability in rainfall (20%<cv<30%), with the Eastern Province and Kigali City being in the largest range (between 25.9 and 27. 3%). The variability of mean temperature was low (cv<10%) and unequally distributed in the study area. There was medium variability of NDVI in the study area with unequal distribution.

During 2024-2053, the highest variability in rainfall will be at Ruhengeri and Bigogwe in the Northern Province under RCP 2.6 and the smallest medium-range variability in rainfall will be in the southwest of the Southern Province and the south region of the Western Province. The high-range variability in average annual rainfall will dominate the southern part of the Southern Province and Western Province whereas the medium-range variability will be concentrated in the great part of the Northern Province under RCP 8.5. The average annual mean temperature will show low variability in the study area but that variability will be generally larger under RCP 8.5 than under RCP 2.6. The NDVI also will fall in low-range variability changing from region to region in the study area.

The correlation of NDVI to either rainfall or mean temperature was unequally distributed in the study area with a low positive or negative coefficient of correlation**.** However**,** the NDVI was more correlated to mean temperature than rainfall in different regions of the study area during the 1983-2020 period. This will be the same under the two scenarios in consideration during the 2024-2053 period. Because of the considerable correlation between the NDVI and both rainfall and temperature, the monitoring of the vegetation cover should take into account and control the factors that can fluctuate such climate variables.

While the NDVI showed decreasing significant trends at Gitega, Cyato at the same rate of $-0.0006 year^{-1}$ and the respective increasing significant trend at Butare, Gikonko, Musambira, Kabgayi, Busasamana, Muganza, Byimana, Gisenyi, Bugarama and Karangazi with slopes of $0.0060 year^{-1}$, $0.0085 year^{-1}$ **,** $0.0084 year^{-1}$ **,** $0.0079 year^{-1}$ **,** $0.0099 year^{-1}$**,** $0.0058 year^{-1}$ **,** $0.0271 year^{-1}$**,** $0.0001 year^{-1}$**,** $0.0100 year^{-1}$**,** and $0.0271 year^{-1}$ during the 1983-2020 period will be the existence of the trends of NDVI under the two scenarios at all stations in consideration with insignificantly increasing except at Cyato where there will be an insignificantly decreasing trend with a slope of $2.4E$ - 05 $year^{-1}$ under RCP 2.6. Under RCP 8.5, there will be significant increasing trends except at Musambira, Gikongoro, Muganza, Cyinzuzi, Kinoni, and Murunda where the trends will be insignificantly increasing.

In addition to the Normalized Difference Vegetation Index (NDVI), for further monitoring of the vegetation cover in Rwanda other studies should consider more indices such as ratio vegetation index (RVI), Green vegetation index (GVI), leaf area index (LAI), enhanced vegetation index (EVI) to relate them with climate

factors both at annual scale and seasonal scale. One should also consider the contribution of topography and demography to vegetation cover status.

ADDENDUM ONE: LIST OF FIGURES

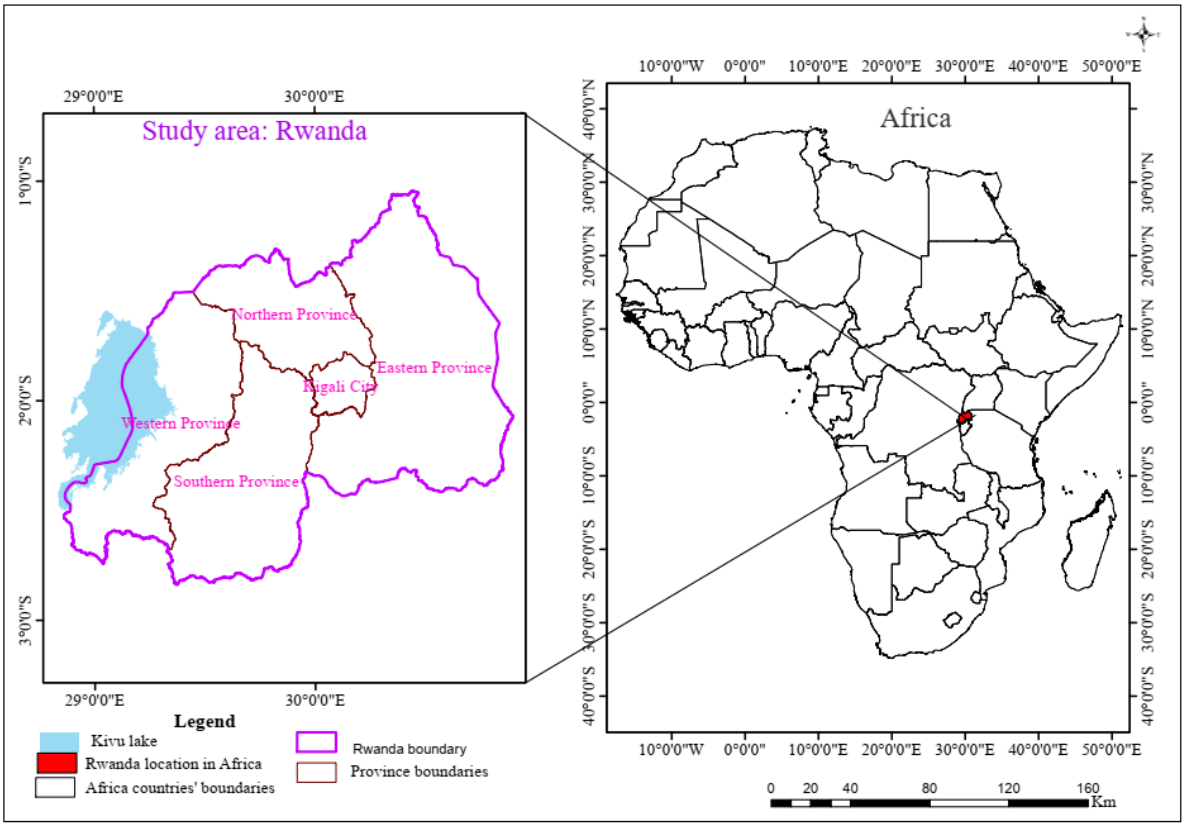

Figure 1: Map of the study area

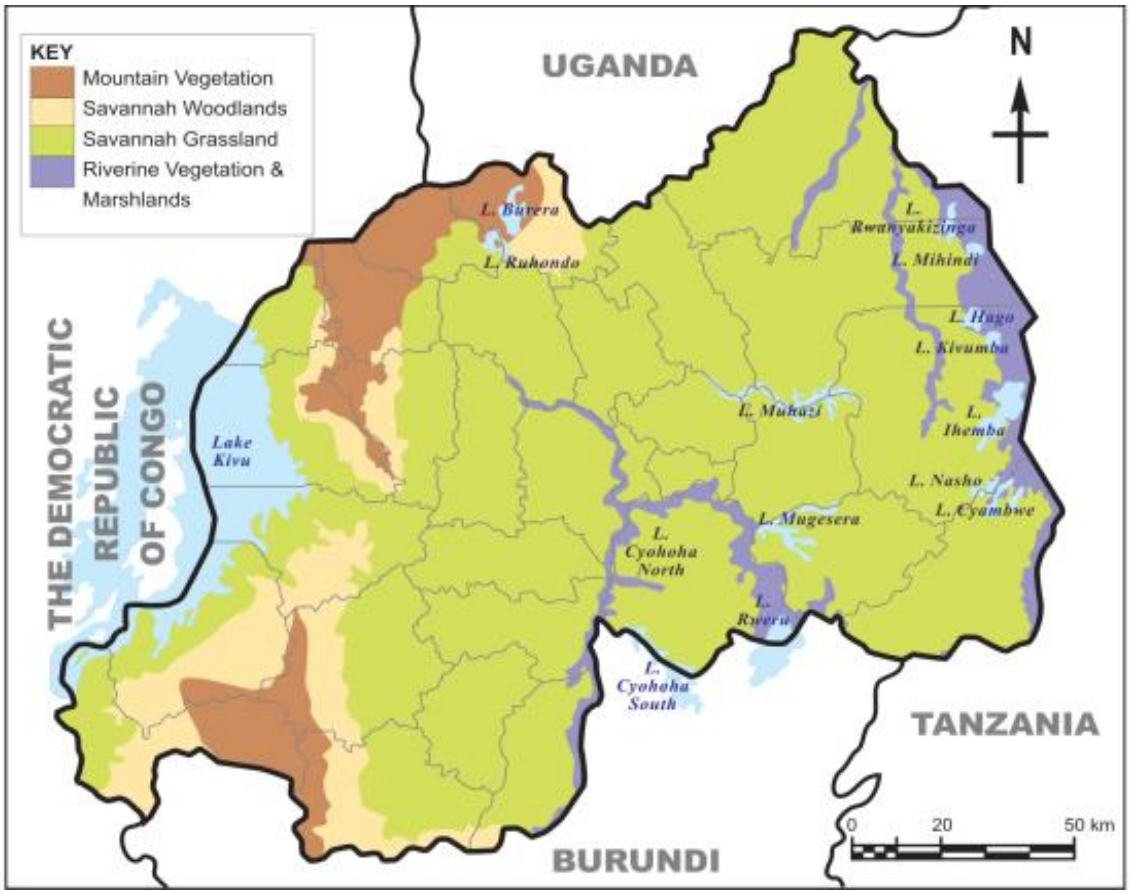

Figure 2:Map of regions of natural vegetation in Rwanda

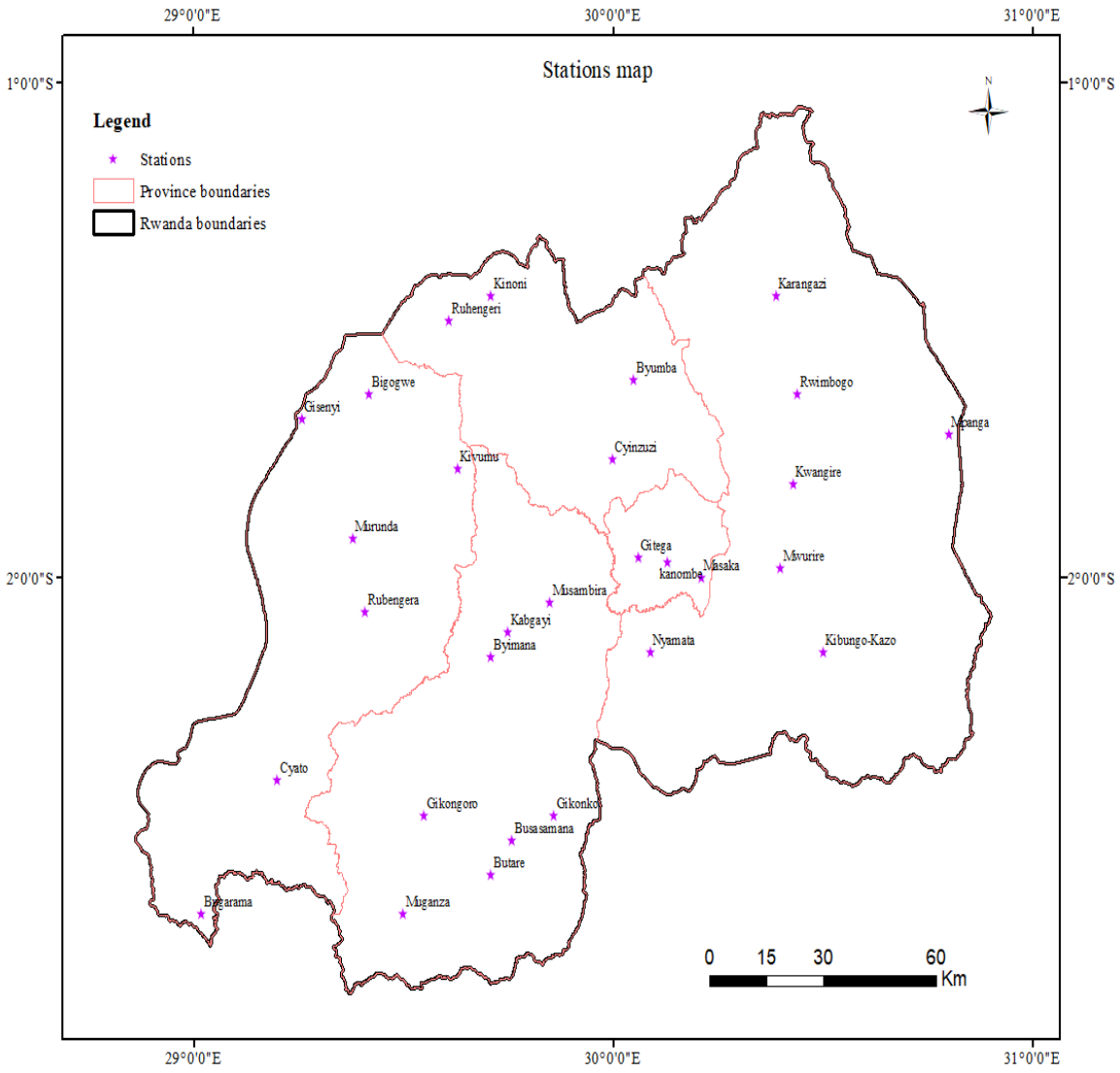

Figure 3: Map of meteo stations used in this study

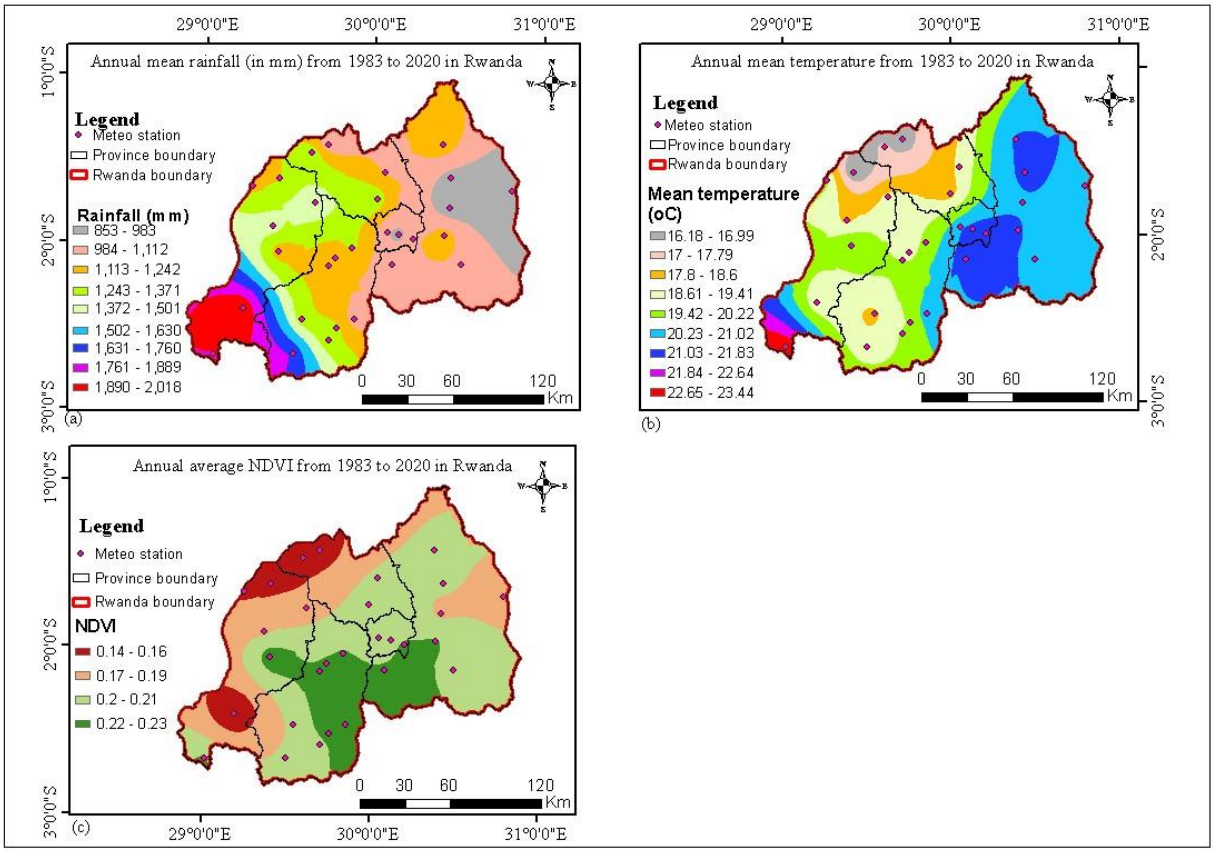

Figure 4: Spatial distribution of average annual (a) rainfall,(b) mean temperature, and (c) NDVI from 1983 to 2020 in Rwanda.

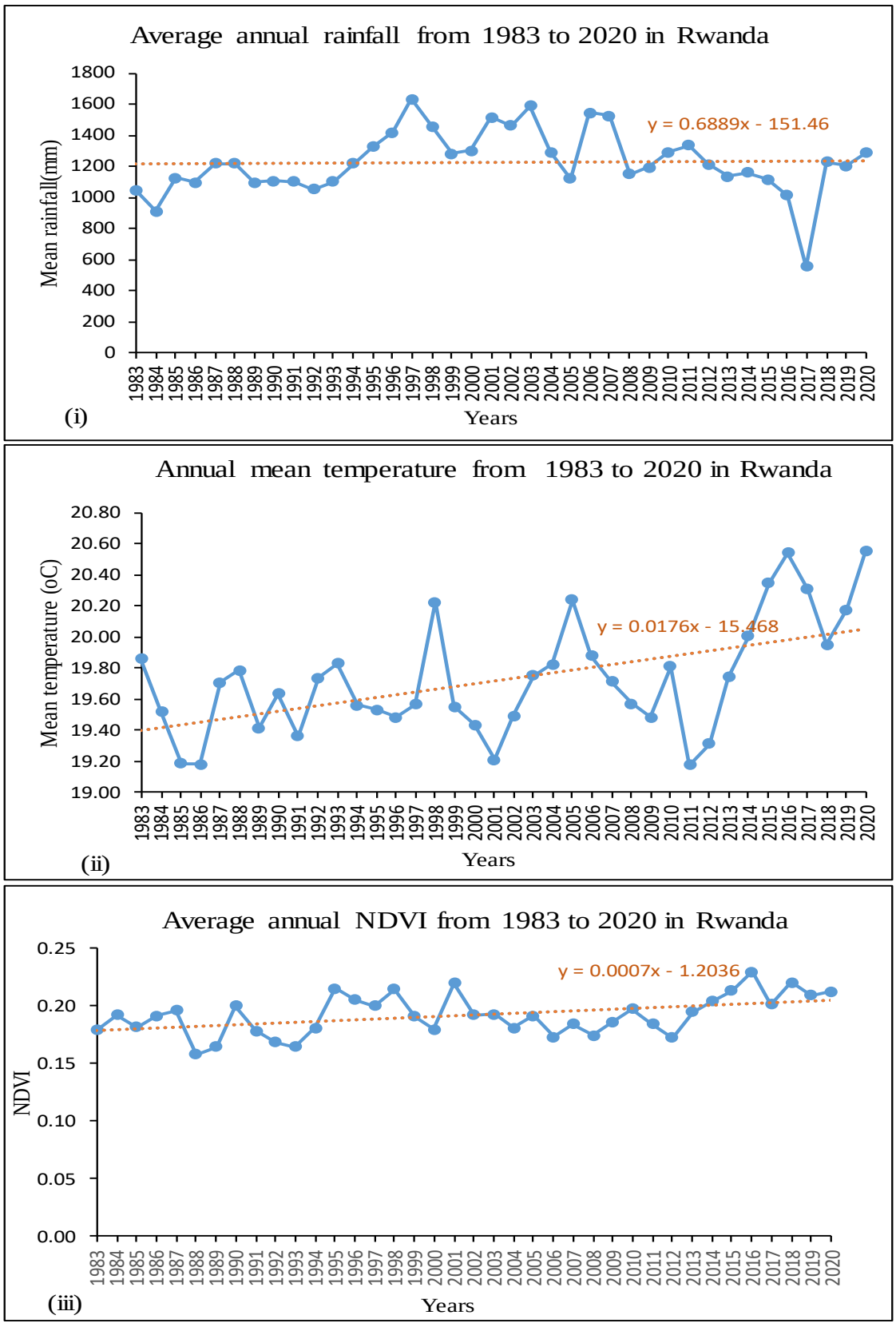

Figure 5*:* Temporal variations of (i)average annual rainfall, (ii) average annual mean temperature, and (ii) average annual NDVI in Rwanda from 1983 to 2020**.**

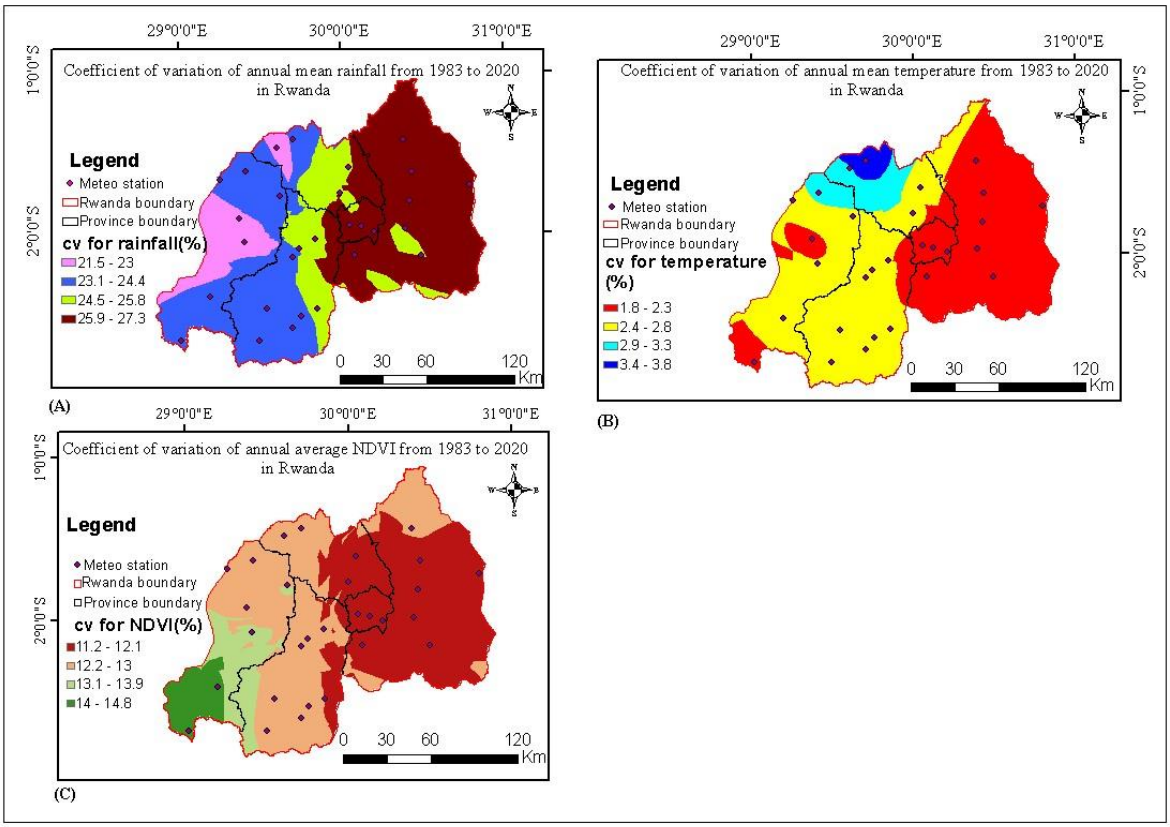

Figure 6: Spatial coefficient of variation of (A) average annual rainfall, (B) average annual mean temperature, and (C) average annual NDVI in Rwanda from 1983 to 2020.

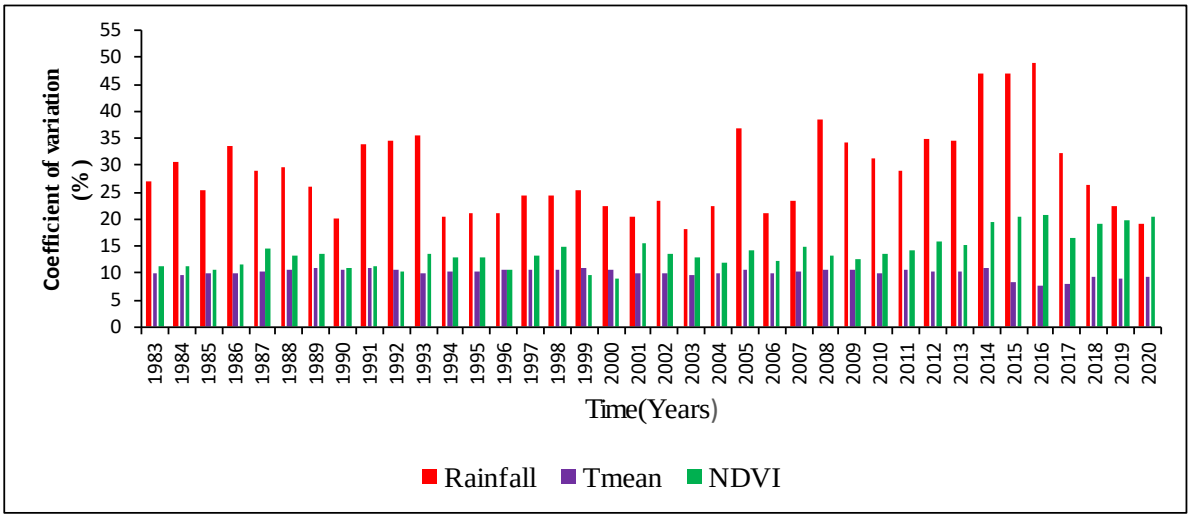

Figure 7: Temporal coefficient of variation of average annual rainfall, average annual mean temperature, and average annual NDVI in Rwanda from 1983 to 2020.

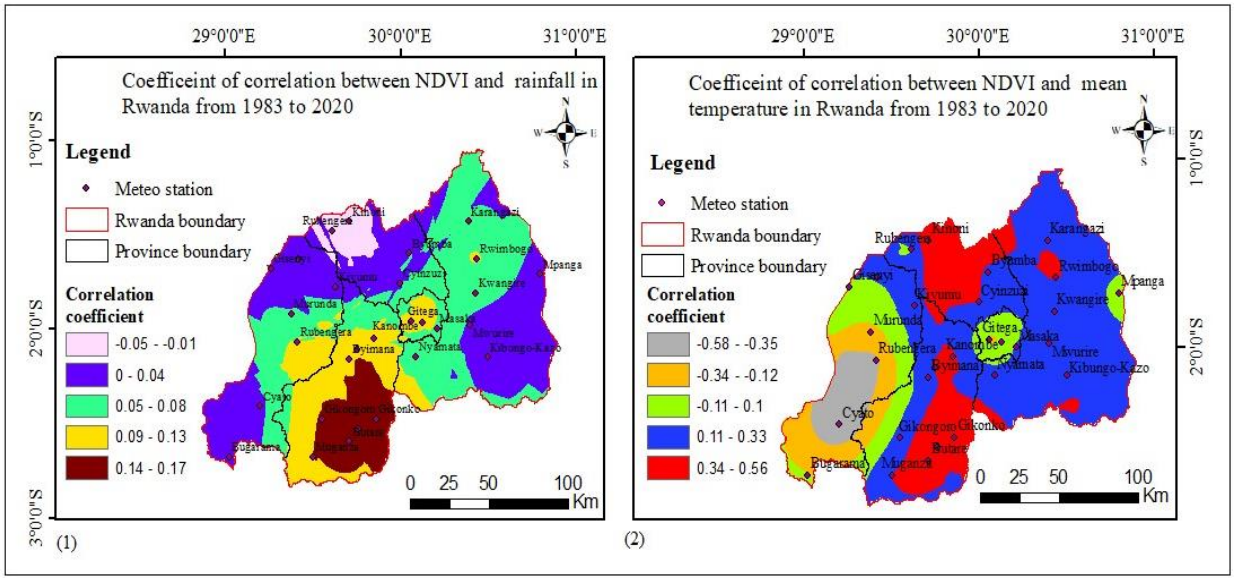

Figure 8: Spatial coefficient of correlation between average annual NDVI and (1) average annual rainfall, (2) average annual temperature from 1983 to 2020

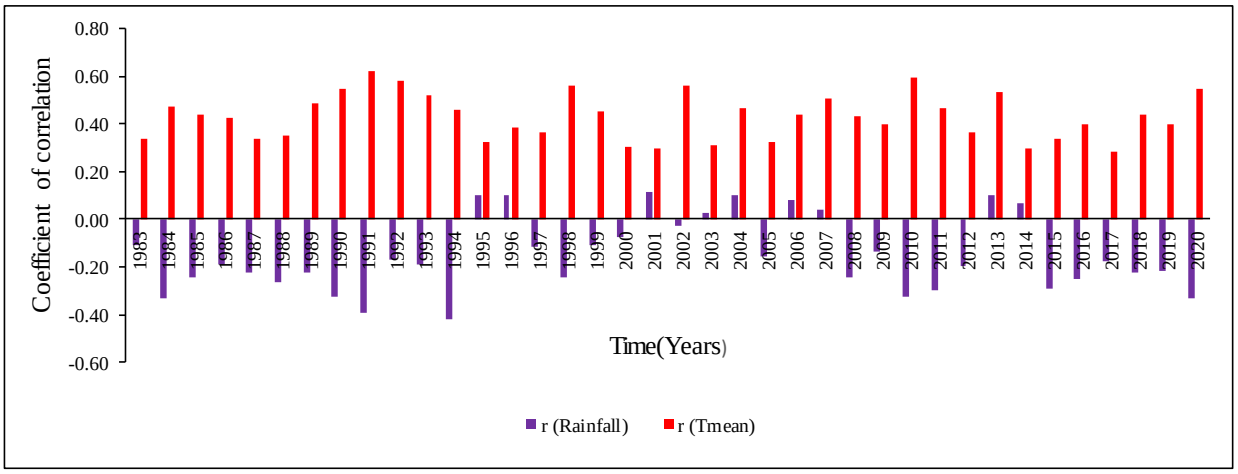

Figure 9: Temporal correlation coefficient NDVI and average annual rainfall, r (Rainfall) and average annual mean temperature, r (Tmean) from 1983 to 2020 in Rwanda.

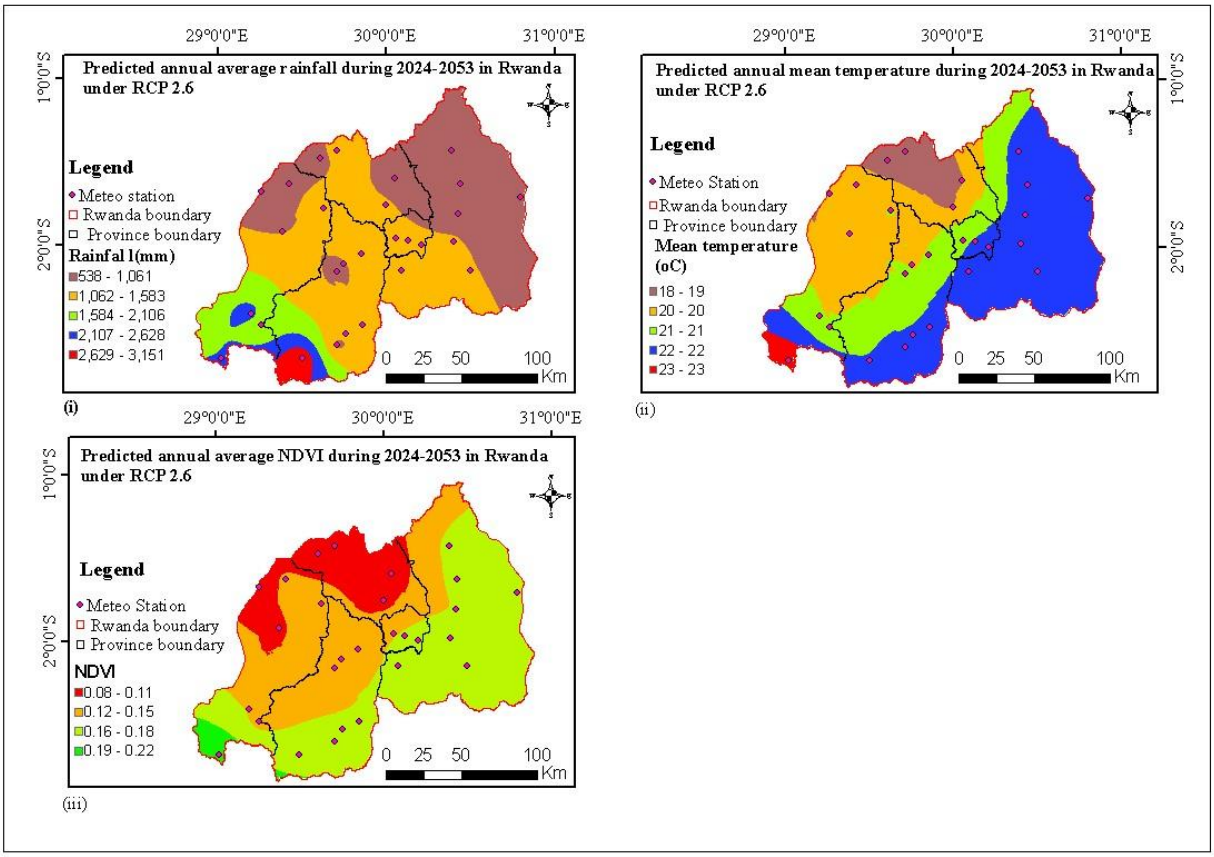

Figure 10:Spatial distribution of predicted (i) average annual rainfall,(ii) average annual mean temperature, and (iii) average annual NDVI under RCP2.6 during 2024-2053 in Rwanda.

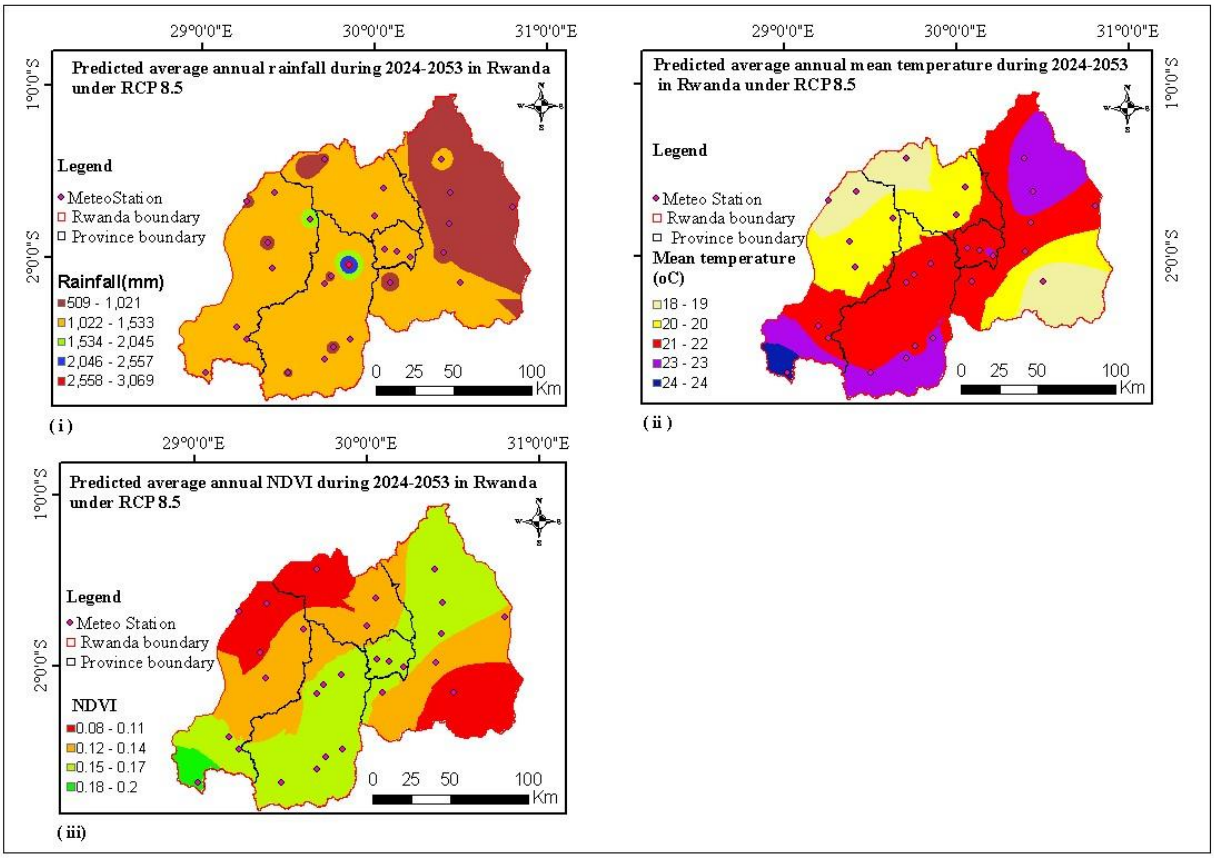

Figure 11:Spatial distribution of predicted (i) average annual rainfall,(ii) average mean temperature,(iii) average annual NDVI under RCP8.5 during 2024-2053 in Rwanda.

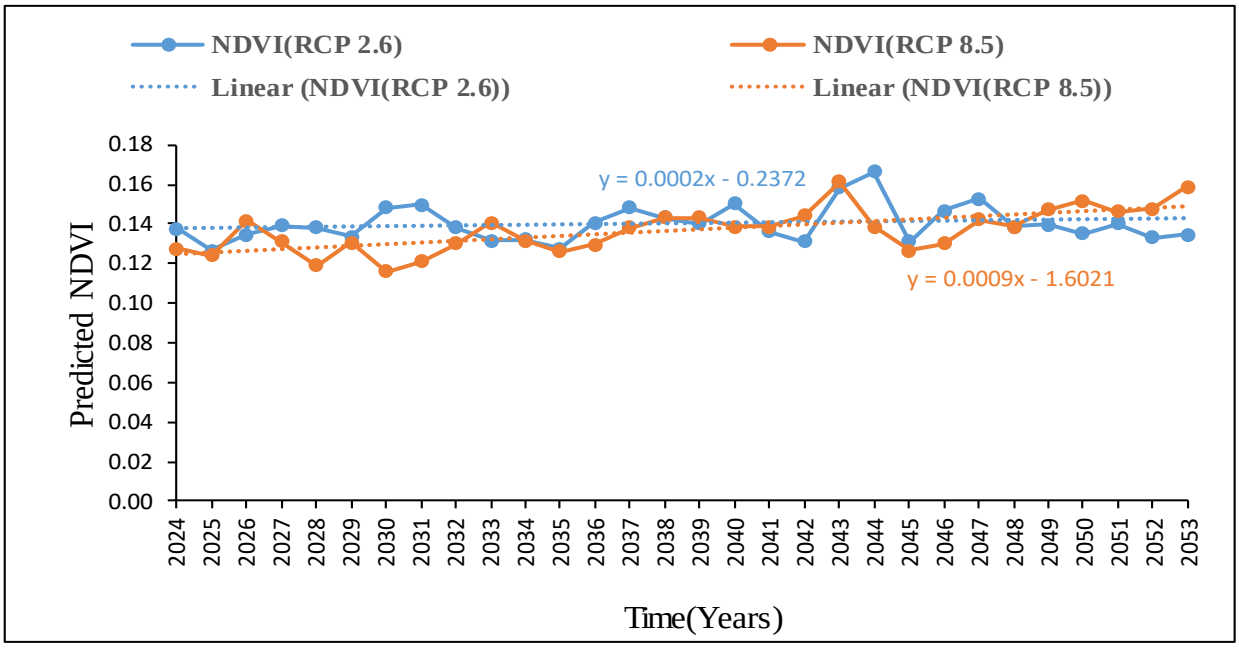

Figure 12: Temporal variability of NDVI during 2024-2053 under RCP2.6 and RCP 8.5

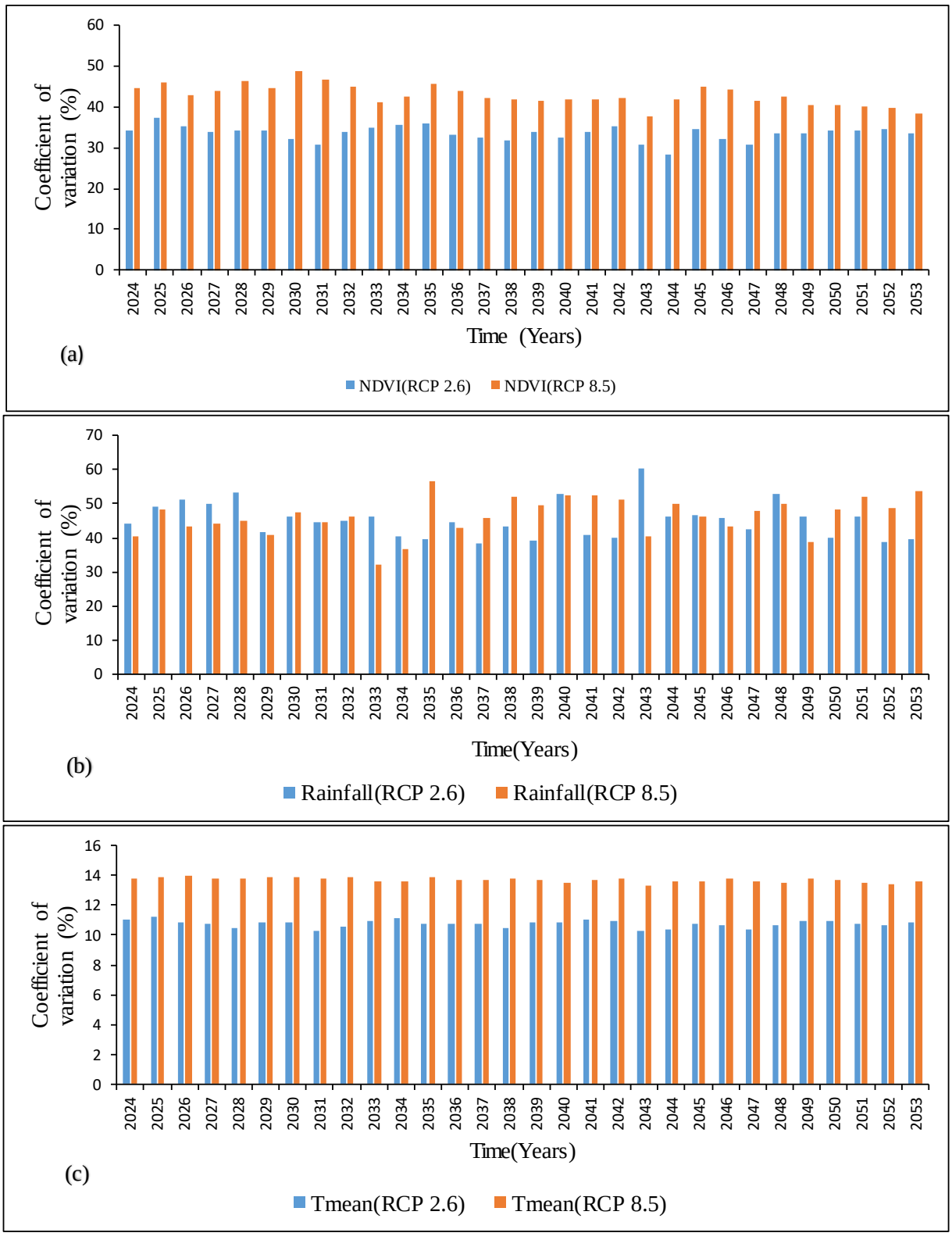

Figure 13: Temporal coefficient of variation of (a) predicted average annual rainfall, (b) annual mean temperature, and average annual (c)NDVI during 2024-2053 under RCP2.6 and RCP 8.5 in Rwanda

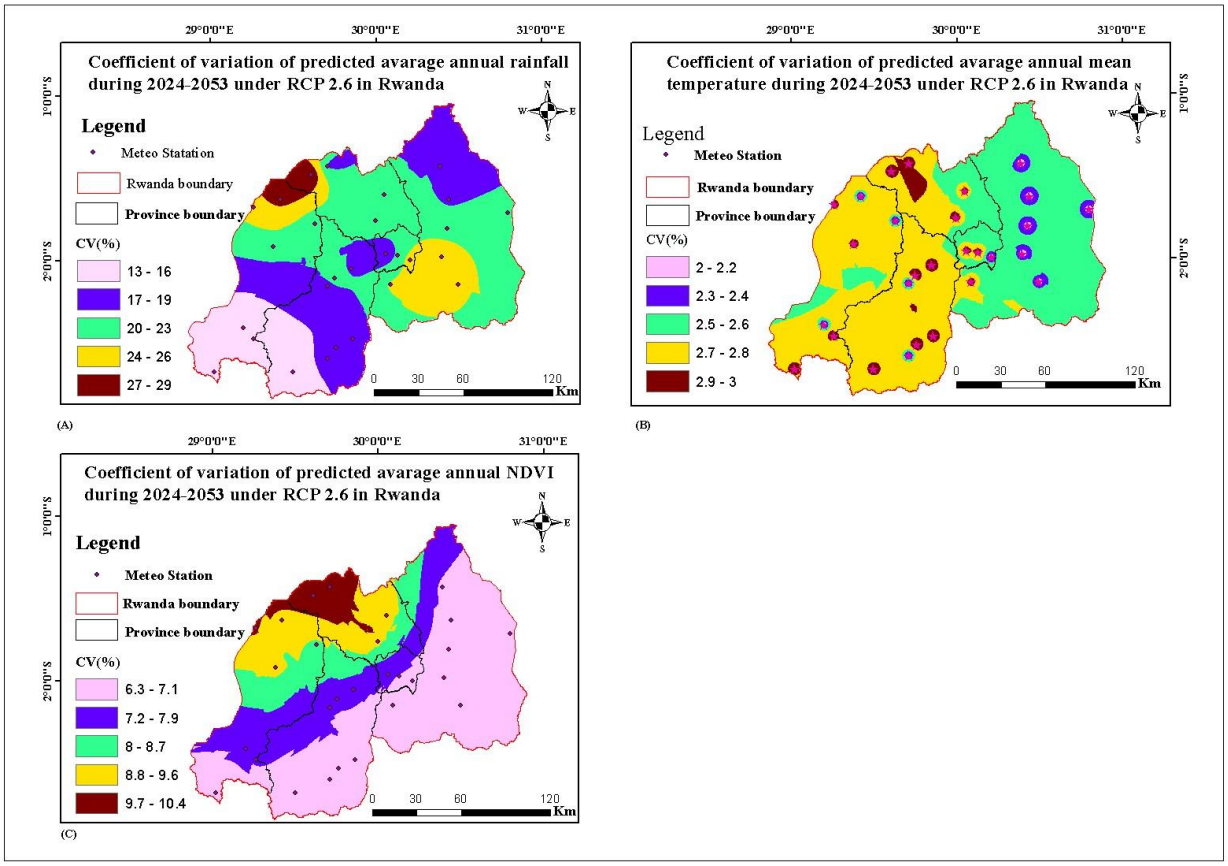

Figure 14: Spatial coefficient of variation of predicted (A) average annual rainfall, (B) average annual mean temperature, and (C) average annual NDVI during 2024-2053 under RCP2.6 in Rwanda.

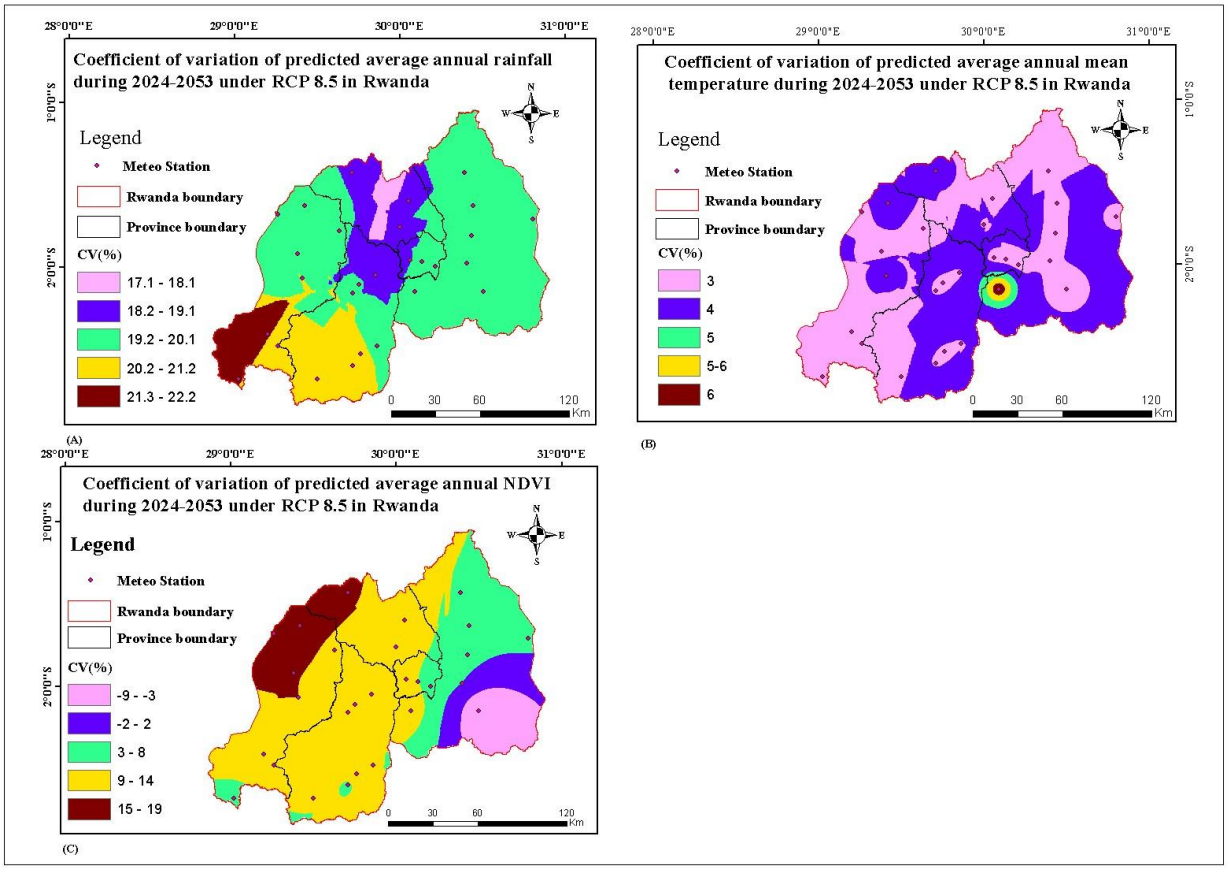

Figure 15: Spatial coefficient of variation of predicted (A) average annual rainfall, (B) average annual mean temperature, and (C) average annual NDVI during 2024-2053 under RCP 8.5 in Rwanda.

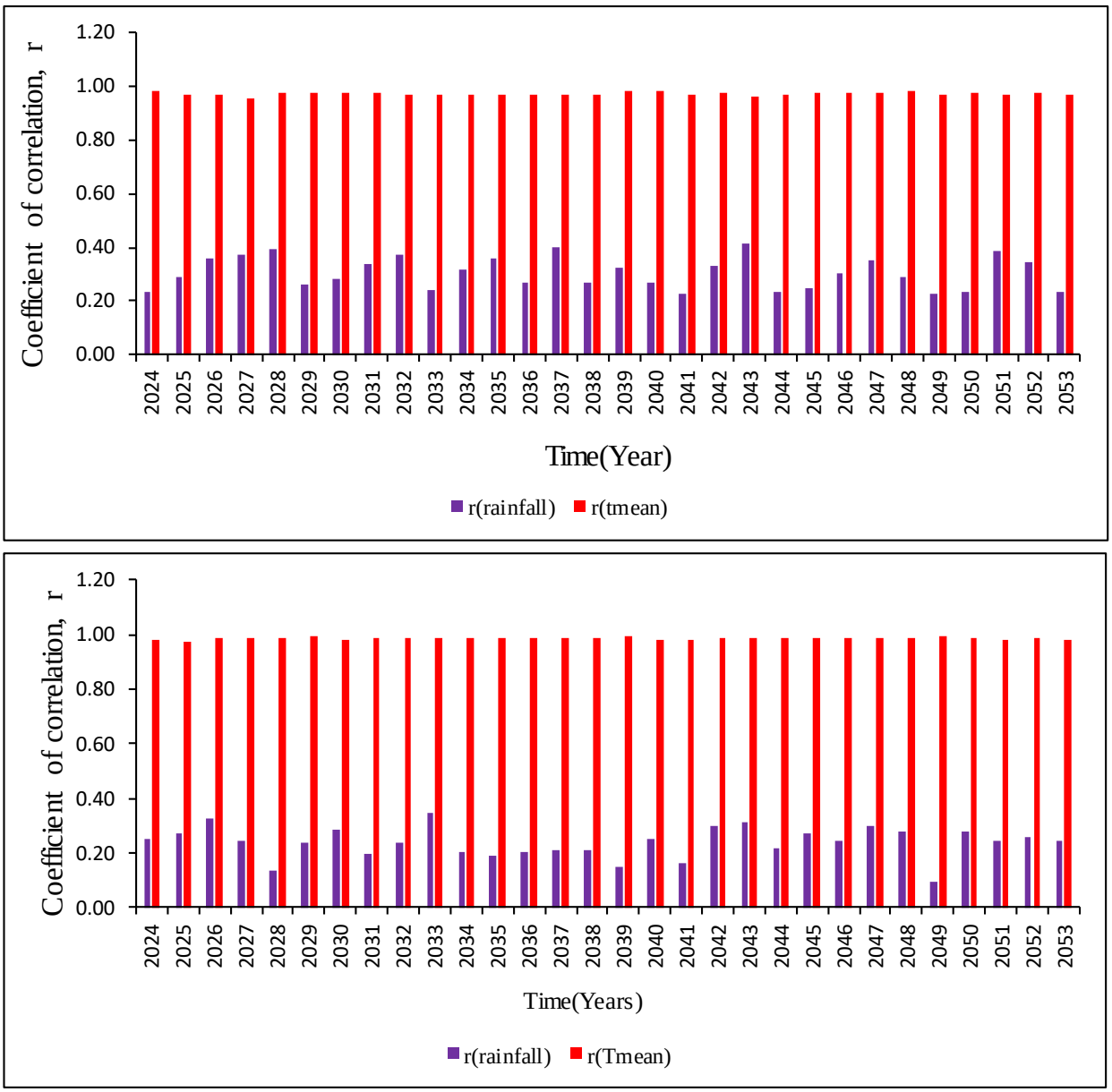

Figure 16: Temporal coefficient of correlation (r) between predicted average NDVI and predicted average annual rainfall and average annual mean temperature during 2023-2024 under RCP2.6(above) and RCP 8.5 (below) in Rwanda.

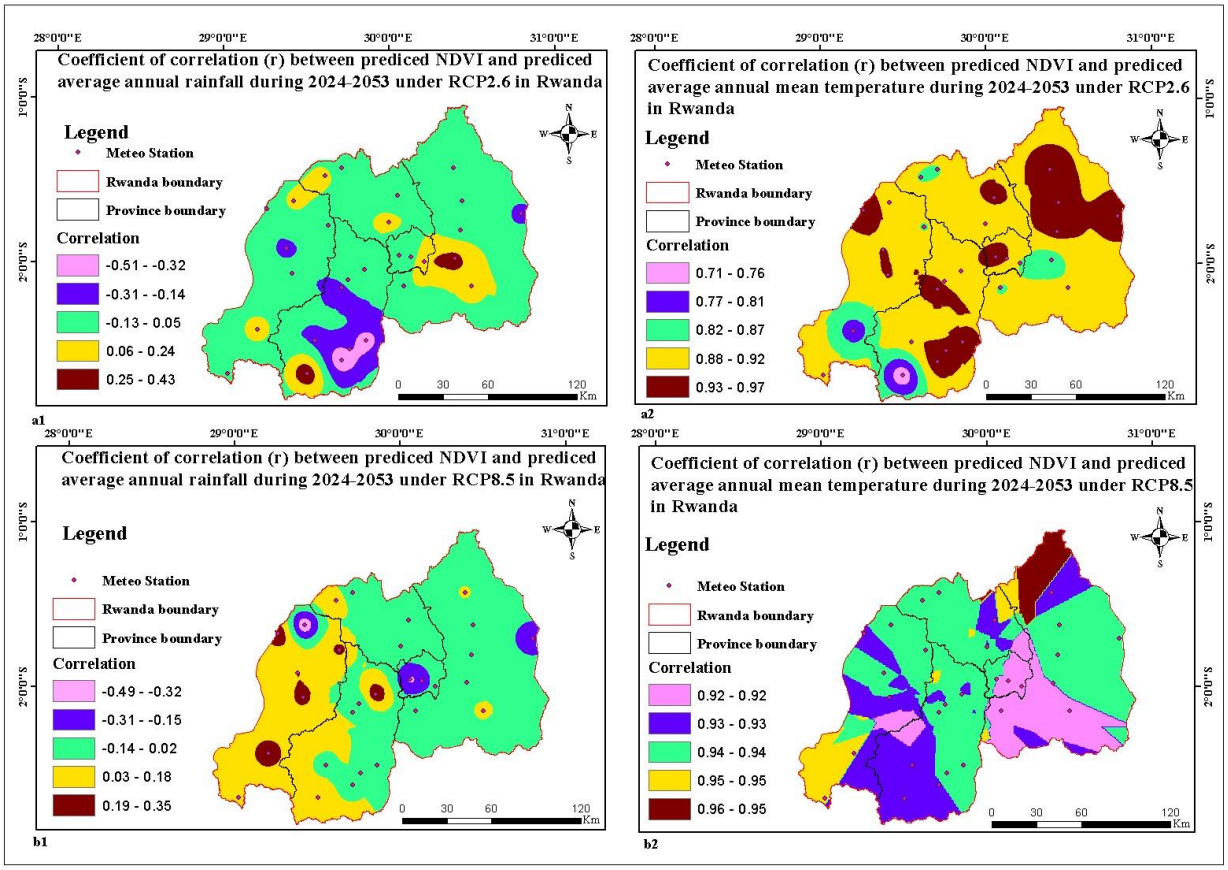

Figure 17: Spatial coefficient of correlation (r) between predicted average NDVI and predicted average annual rainfall, average annual mean temperature during 2023-2024 under RCP 2.6 and RCP 8.5 in Rwanda.

ADDENDUM TWO: LIST OF TABLES

Table 1:List of meteorology stations used and their respective coordinates by District in Rwanda

No	Stations	Longitude (Degrees)	Latitude (Degrees)	Altitude (m)	District
1	Gitega	30.06	-1.96	1522	Nyarygenge
2	Kanombe	30.13	-1.97	1474	Kicukiro
3	Masaka	30.21	-2	1549	Kicukiro
4	Gikonko	29.86	-2.48	1493	Gisagara
5	Butare	29.71	-2.6	1691	Huye
6	Musambira	29.85	-2.05	1657	Kamonyi
7	Kabgayi	29.75	-2.11	1794	Muhanga
8	Gikongoro	29.55	-2.48	2022	Nyamagabe
9	Busasamana	29.76	-2.53	1733	Nyanza
10	Muganza	29.5	-2.68	1937	Nyaruguru
11	Byimana	29.71	-2.16	1778	Ruhango
12	Cyinzuzi	30	-1.76	2036	Rilindo
13	Kinoni	29.71	-1.43	2105	Burera
14	Byumba	30.05	-1.6	2207	Gicumbi
15	Ruhengeri	29.61	-1.48	1967	Musanze
16	Rubengera	29.41	-2.07	1613	Karongi
17	Kivumu	29.63	-1.78	1960	Ngororero
18	Bigogwe	29.42	-1.63	2370	Nyabihu
19	Cyato	29.2	-2.41	1650	Nyamasheke
20	Gisenyi	29.26	-1.68	1541	Rubavu
21	Bugarama	29.02	-2.68	956	Rusizi
22	Murunda	29.38	-1.92	1776	Rutsiro
23	Rwimbogo	30.44	-1.63	1426	Gatsibo
24	Nyamata	30.09	-2.15	1435	Bugesera
25	Mwurire	30.4	-1.98	1605	Rwamagagna
26	Mpanga	30.8	-1.71	1303	Kirehe
27	Kwangire	30.43	-1.81	1523	Kayonza
28	Kibungo-Kazo	30.5	-2.15	1446	Ngoma
29	Karangazi	30.39	-1.43	1399	Nyagatare

Table 2*:* Ranges of NDVI values

Vegetation type	NDVI class	Range of NDVI values
No vegetation (cloud, water)	No vegetation	< 0
Barren rock or bare soil, sand, snow	Low	$0 - 0.1$
Sparse vegetation (shrubs, grasslands)	Moderate	$0.2 - 0.5$
Dense vegetation	High	$0.6 - 0.9$

Table 3*:*Ranges of coefficient of variation

Pearson correlation coefficient range	Implication
$0 - \pm 0.19$	Very low positive/negative correlation
$\pm 0.2 - \pm 0.39$	Low positive/negative correlation
$\pm 0.4 - \pm 0.59$	Moderate positive/negative correlation
$\pm 0.6 - \pm 0.79$	High positive/negative correlation
$\pm 0.8 - \pm 0.9$	Very high positive/negative correlation

Table 4: Mann-Kendall statistics for average annual mean temperature, average annual rainfall, and average annual NDVI in Rwanda during 1983-2020

	Mean tempearture				Rainfall				NDVI			
Station	Ts	μ	P-value	Signif.	Ts	μ	P-value	Signif.	Ts	μ	P-value	Signif.
Gitega	1.766	0.008	0.077		-0.248	-0.644	0.804		-2.3150	-0.00069	0.0206	*
kanombe	2.315	0.012	0.021	*	-0.222	-0.979	0.824		-0.5885	-0.00023	0.5562	
Masaka	1.739	0.013	0.082		0.144	-0.979	0.886		0.8240	0.00023	0.4100	
Gikonko	2.498	0.016	0.012	*	-0.301	-1.469	0.764		2.1580	0.00085	0.0309	*
Butare	2.341	0.012	0.019	*	0.641	2.990	0.522		2.0272	0.00060	0.0426	*
Musambira	2.917	0.014	0.004	*	0.039	0.506	0.969		2.1842	0.00084	0.0289	*
Kabgayi	2.969	0.015	0.003	*	0.170	0.851	0.865		2.2626	0.00079	0.0237	*
Gikongoro	1.530	0.008	0.126		1.426	6.075	0.154		1.5302	0.00054	0.1260	
Busasamana	2.446	0.018	0.014	*	0.013	0.117	0.990		2.2365	0.00099	0.0253	*
Muganza	1.766	0.009	0.077		-0.039	-0.265	0.969		2.7596	0.00062	0.0058	*
Byimana	1.766	0.009	0.077		-0.719	-2.591	0.472		2.2103	0.00073	0.0271	*
Cyinzuzi	1.923	0.009	0.055		-0.562	-3.438	0.574		1.1640	0.00042	0.2444	
Kinoni	1.190	0.007	0.234		-0.981	-3.890	0.327		1.0332	0.00031	0.3015	
Byumba	2.027	0.010	0.043	*	1.138	3.579	0.255		1.6087	0.00056	0.1077	
Ruhengeri	2.367	0.011	0.018	*	0.144	0.689	0.886		0.4578	0.00008	0.6471	
Rubengera	0.000	0.000	1.000		1.164	1.164	1.164		1.7395	0.00096	0.0819	
Kivumu	2.760	0.015	0.006	*	1.164	1.164	1.164		0.9024	0.00039	0.3668	
Bigogwe	1.674	0.010	0.094		1.164	0.623	0.623		-0.4578	-0.00013	0.6471	
Cyato	2.393	0.013	0.017	*	1.504	5.432	0.133		-2.2626	-0.00069	0.0237	*
Gisenyi	1.347	0.007	0.178		1.766	7.244	0.077		0.8915	0.00015	0.0001	*
Bugarama	0.248	0.001	0.804		-1.216	-5.589	0.224		2.5765	0.00099	0.0100	*
Murunda	0.301	0.002	0.764		1.007	4.132	0.314		1.5995	0.00057	0.1097	
Rwimbogo	2.289	0.011	0.022	*	2.080	6.230	0.038	*	0.7455	0.00438	0.4560	
Nyamata	2.263	0.012	0.024	*	-1.478	-4.758	0.139		0.8501	0.00029	0.3953	
Mwurire	1.923	0.010	0.055		-0.510	-2.019	0.610		0.1177	0.00004	0.9063	
Mpanga	1.216	0.006	0.224		1.216	3.339	0.224		0.9024	0.00015	0.3668	
Kwangire	1.347	0.007	0.178		0.641	0.641	0.522		0.1177	0.00005	0.9063	
Kibungo-Ka	2.472	0.012	0.013	*	-0.432	-1.071	0.666		0.4054	0.00015	0.6852	
Karangazi	1.661	0.008	0.097		1.556	4.658	0.120		2.2103	0.00082	0.0271	*

Table 5: Spatial and temporal coefficient of correlation (r) of NDVI with either average annual rainfall or annual mean temperature for 29 stations in Rwanda from 1983 to 2020.

	Spatial		**Temporal**		
	Rainfall	Tmean		Rainfall	Tmean
Stations	**r**	**r**	**Year**	**r**	**r**
Gitega	0.3	-0.22	**1983**	-0.11	0.34
Kanombe	0.36	-0.15	**1984**	-0.34	0.47
Masaka	0.07	0.17	**1985**	-0.25	0.44
Gikonko	0.15	0.46	**1986**	-0.19	0.43
Butare	0.2	0.42	**1987**	-0.22	0.34
Musambira	0.15	0.39	**1988**	-0.27	0.35
Kabgayi	0.07	0.4	**1989**	-0.22	0.49
Gikongoro	0.2	0.2	**1990**	-0.32	0.55
Busasamana	0.21	0.6	**1991**	-0.39	0.62
Muganza	0.25	0.36	**1992**	-0.17	0.58
Byimana	0.1	0.21	**1993**	-0.19	0.52
Cyinzuzi	-0.11	0.38	**1994**	-0.42	0.46
Kinoni	-0.38	0.64	**1995**	0.1	0.32
Byumba	-0.02	0.29	**1996**	0.1	0.39
Ruhengeri	0.16	0.01	**1997**	-0.11	0.36
Rubengera	0.23	-0.42	**1998**	-0.25	0.56
Kivumu	-0.01	0.29	**1999**	-0.11	0.45
Bigogwe	0	0.13	**2000**	-0.07	0.3
Cyato	-0.12	-0.63	**2001**	0.12	0.3
Gisenyi	0.09	0.1	**2002**	-0.03	0.56
Bugarama	-0.2	-0.11	**2003**	0.03	0.31
Murunda	-0.06	-0.21	**2004**	0.1	0.47
Rwimbogo	0.33	0.38	**2005**	-0.15	0.32
Nyamata	-0.18	0.21	**2006**	0.08	0.44
Mwurire	-0.09	0.28	**2007**	0.04	0.51
Mpanga	-0.06	0.04	**2008**	-0.25	0.43
Kwangire	0	0.11	**2009**	-0.14	0.4
Kibungo-Kaz	-0.03	0.28	**2010**	-0.33	0.59
Karangazi	0.06	0.32	**2011**	-0.3	0.46
			2012	-0.2	0.37
			2013	0.1	0.53
			2014	0.07	0.3
			2015	-0.29	0.34
			2016	-0.25	0.4
			2017	-0.18	0.28
			2018	-0.22	0.44
			2019	-0.22	0.4
			2020	-0.33	0.55

Table 6:Man-Kendall statistics of predicted average annual NDVI under RCP 2.6 and RCP8.5 for 29 stations in Rwanda during 2024-2053

Station	NDVI(RCP2.6)				NDVI(RCP8.5)			
	Ts	$\mu(°C\ year^{-1})$	P-value	Signif.	Ts	$\mu(°C\ year^{-1})$	P-value	Signif.
Gitega	0.1501	1.78E-05	0.88		2.67607	0.0006	0.01	*
kanombe	0.5065	0.0001	0.61		2.4838	0.0005	0.01	*
Masaka	0.2814	5.92E-05	0.78		2.09895	0.0005	0.04	*
Gikonko	0.2439	7.46E-05	0.81		2.24728	0.0005	0.02	*
Butare	0.4127	9.14E-05	0.68		2.07967	0.0004	0.04	*
Musambira	0.6192	8.26E-05	0.54		1.67696	0.0005	0.09	
Kabgayi	0.4314	0.0001	0.67		2.15197	0.0005	0.03	*
Gikongoro	0.6190	9.99E-05	0.54		1.7776	0.0005	0.08	
Busasamana	0.1501	3.12E-05	0.88		2.05429	0.0005	0.04	*
Muganza	0.7691	0.0002	0.44		1.75046	0.0005	0.08	
Byimana	0.1126	3.68E-05	0.91		2.62	0.0005	0.01	*
Cyinzuzi	0.8816	0.0001	0.38		1.12659	0.0002	0.26	
Kinoni	1.2943	0.0002	0.20		1.6959	0.0004	0.09	
Byumba	0.7505	0.0001	0.45		1.98337	0.0003	0.05	*
Ruhengeri	0.9942	0.0002	0.32		1.98953	0.0005	0.05	*
Rubengera	0.4690	8.64E-05	0.64		2.48409	0.0007	0.01	*
Kivumu	0.9567	0.0002	0.34		3.00585	0.0007	0.00	*
Bigogwe	0.9191	0.0002	0.36		1.98196	0.0004	0.05	*
Cyato	-0.1688	-2.4E-05	0.87		2.61536	0.0006	0.01	*
Gisenyi	0.4690	0.0001	0.64		2.61721	0.0008	0.01	*
Bugarama	0.6565	0.0002	0.51		2.1817	0.0007	0.03	*
Murunda	0.7691	0.0001	0.44		1.6945	0.0005	0.09	
Rwimbogo	0.5440	0.0001	0.59		2.15299	0.0005	0.03	*
Nyamata	0.6754	8.97E-05	0.50		3.04588	0.0005	0.00	*
Mwurire	0.3939	7.52E-05	0.69		2.48644	0.0006	0.01	*
Mpanga	0.5815	7.04E-05	0.56		2.7409	0.0004	0.01	*
Kawangire	0.3002	6.43E-05	0.76		2.78735	0.0004	0.01	*
Kibungo	0.2814	2.78E-05	0.78		2.53234	0.0003	0.01	*
Karangazi	0.2251	5.96E-05	0.82		2.30408	0.0005	0.02	*

Table 7: Man-Kendall statistics of predicted average annual rainfall under RCP 2.6 and RCP8.5 for 29 stations in Rwanda during 2024-2053.

Station	Rainfall(RCP2.6)				Rainfall(RCP8.5)			
	Ts	$\mu(°C\ year^{-1})$	P-value	Signif.	Ts	$\mu(°C\ year^{-1})$	P-value	Signif.
Gitega	0.02122	5.4963	0.15		-1.107	-3.7221	0.2684	
kanombe	1.18176	0.2515	0.24		-1.294	-3.2737	0.1956	
Masaka	1.18176	4.2515	0.24		0.2063	0.5830	0.8365	
Gikonko	0.43144	2.2454	0.67		-1.107	-2.5838	0.2684	
Butare	-1.4069	-5.9003	0.16		-1.519	-5.5552	0.1287	
Musambira	-1.3693	-4.9628	0.17		-0.319	-4.7030	0.7498	
Kabgayi	0.39392	1.6614	0.69		-1.294	-4.4377	0.1956	
Gikongoro	0.3564	1.7629	0.72		-0.394	-3.0498	0.6936	
Busasamana	-0.544	-2.6543	0.59		-1.407	-4.2980	0.1595	
Muganza	-0.9942	-5.0306	0.32		-0.882	-3.5514	0.378	
Byimana	0.20634	2.3700	0.84		-1.82	-5.6258	0.0688	
Cyinzuzi	-0.0563	-0.2833	0.96		-2.27	-9.2589	0.0232	*
Kinoni	1.21927	4.5157	0.22		-1.707	-5.8308	0.0878	
Byumba	0.46895	1.7787	0.64		-2.045	-7.0643	0.0409	*
Ruhengeri	0.99418	3.5771	0.32		-0.957	-1.8809	0.3387	
Rubengera	0.09379	0.4089	0.93		-0.657	-2.9756	0.5115	
Kivumu	-0.8441	-4.0928	0.40		-0.619	-3.7272	0.5359	
Bigogwe	0.20634	1.3030	0.84		-2.645	-7.3823	0.0082	*
Cyato	0.69405	2.8675	0.49		-0.694	-4.9245	0.4877	
Gisenyi	1.06921	1.8183	0.28		1.2943	-5.9384	0.1956	
Bugarama	-0.7316	-7.4640	0.46		-1.557	-8.1979	0.1195	
Murunda	0.09379	0.1274	0.93		-1.069	-1.0692	0.285	
Rwimbogo	1.10673	3.3050	0.27		-1.482	-5.8330	0.1384	
Nyamata	0.54398	2.0621	0.59		-1.294	-4.1489	0.1956	
Mwurire	0.3564	2.6053	0.72		-0.581	-1.3447	0.5609	
Mpanga	0.8066	2.3313	0.42		-1.182	-3.3721	0.2373	
Kawangire	0.24385	0.9771	0.81		-0.657	-2.9892	0.5115	
Kibungo	0.31889	0.8434	0.75		-0.431	-1.8913	0.6662	
Karangazi	2.15718	6.8739	0.03	*	-0.094	-0.5604	0.9253	

Table 8: Man-Kendall statistics of predicted average annual mean temperature under RCP 2.6 and RCP8.5 for 29 stations in Rwanda during 2024-2053.

Station	Tmean(RCP2.6)				Tmean(RCP8.5)			
	Ts	$\mu(°C\ year^{-1})$	P-value	Signif.	Ts	$\mu(°C\ year^{-1})$	P-value	Signif.
Gitega	0.0563	0.0011	0.96		1.8946	0.0246	0.06	
kanombe	0.0188	0.0010	0.99		1.9321	0.0248	0.05	
Masaka	-0.094	-0.0013	0.93		2.0071	0.0212	0.04	*
Gikonko	0.3189	0.0073	0.75		2.1572	0.0316	0.03	*
Butare	0.4314	0.0076	0.67		2.1947	0.0322	0.03	*
Musambira	0.5065	0.0059	0.61		2.1947	0.0282	0.03	*
Kabgayi	0.544	0.0064	0.59		2.1947	0.0282	0.03	*
Gikongoro	0.3939	0.0070	0.69		2.1572	0.0279	0.03	*
Busasamana	0.6565	0.0068	0.51		2.1947	0.0284	0.03	*
Muganza	0.4314	0.0056	0.67		2.0446	0.0285	0.04	*
Byimana	0.544	0.0064	0.59		2.2322	0.0279	0.03	*
Cyinzuzi	0.1313	0.0031	0.90		1.9696	0.0154	0.05	*
Kinoni	0.1313	0.0018	0.90		2.0821	0.0225	0.04	*
Byumba	0.1313	0.0031	0.90		1.707	0.0209	0.09	
Ruhengeri	0.2439	0.0033	0.81		2.4198	0.0214	0.02	*
Rubengera	0.3939	0.0065	0.69		2.4948	0.0290	0.01	*
Kivumu	0.3189	0.0039	0.75		2.4198	0.0257	0.02	*
Bigogwe	0.2063	0.0023	0.84		2.3823	0.0239	0.02	*
Cyato	0.8066	0.0074	0.42		2.6824	0.0253	0.01	*
Gisenyi	0.1688	0.0024	0.87		2.4198	0.0236	0.02	*
Bugarama	0.7691	0.0136	0.44		2.2697	0.0295	0.02	*
Murunda	0.3189	0.0037	0.75		2.4198	0.0254	0.02	*
Rwimbogo	0.0188	0.0007	0.99		1.9696	0.0227	0.05	*
Nyamata	0.2063	0.0027	0.84		3.3202	0.0324	0.00	*
Mwurire	0.1313	0.0021	0.90		1.9696	0.0225	0.05	*
Mpanga	0.0563	0.0006	0.96		1.782	0.0203	0.07	
Kawangire	0.1313	0.0022	0.90		1.782	0.0201	0.07	
Kibungo	0.1313	0.0018	0.90		1.5944	0.0105	0.11	
Karangazi	0.1313	0.0016	0.90		2.0071	0.0232	0.04	*

REFERENCES

[1] U. Nations, F. Convention, and C. Change, "United Nations Framework Convention on Climate Change," no. February 2011, pp. 1–7, 2014.

[2] N. Joshi *et al.*, "ANALYZING the EFFECT of CLIMATE CHANGE (RAINFALL and TEMPERATURE) on VEGETATION COVER of Nepal USING TIME SERIES MODIS IMAGES," *ISPRS Ann. Photogramm. Remote Sens. Spat. Inf. Sci.*, vol. 4, no. 2/W5, pp. 209–216, 2019, doi: 10.5194/isprs-annals-IV-2-W5-209-2019.

[3] M. O. F. Lands, N. Adaptation, P. Of, and T. O. C. Change, "NAPA-RWANDA," no. December, 2006.

[4] Q. Zhuang, S. Wu, X. Feng, and Y. Niu, "Analysis and prediction of vegetation dynamics under the background of climate change in Xinjiang , China," pp. 1–23, 2020, doi: 10.7717/peerj.8282.

[5] J. Wu and Y. Cheng, "Spatial analysis and model construction of NDVI Based on meteorological data," *MATEC Web Conf.*, vol. 355, p. 03040, 2022, doi: 10.1051/matecconf/202235503040.

[6] F. Ndayisaba *et al.*, "Inter-Annual Vegetation Changes in Response to Climate Variability in Rwanda," *J. Environ. Prot. (Irvine,. Calif).*, vol. 08, no. 04, pp. 464–481, 2017, doi: 10.4236/jep.2017.84033.

[7] V. Nzabarinda, A. Bao, W. Xu, and S. Uwamahoro, "A Spatial and Temporal Assessment of Vegetation Greening and Precipitation Changes for Monitoring Vegetation Dynamics in Climate Zones over Africa," 2021.

[8] Y. M. Ngaga, "Forest Plantations and Woodlots in Tanzania," *African For. Forum Work. Pap. Ser.*, vol. 1, no. 16, 2011, doi: 10.13140/RG.2.1.1360.4724.

[9] B. Arakwiye, J. Rogan, and J. R. Eastman, "Thirty years of forest-cover change in Western Rwanda during periods of wars and environmental policy shifts," *Reg. Environ. Chang.*, vol. 21, no. 2, 2021, doi: 10.1007/s10113-020-01744-0.

[10] S. Ndakize Joseph, N. Frederic, T. Aminadab, and I. Vedaste, "A Statistical Analysis of the Historical Rainfall Data Over Eastern Province in Rwanda," *East African J. Sci. Technol.*, vol. 10, no. 1, pp. 33–52,2020,[Online]. Available: http://eajournal.unilak.ac.rw/EAJSThttp://eajournal.unilak.ac.rw/EAJST

[11] B. Safari, "Trend Analysis of the Mean Annual Temperature in Rwanda during the Last Fifty Two Years," *J. Environ. Prot. (Irvine,. Calif).*, vol. 03, no. 06, pp. 538–551, 2012, doi:

10.4236/jep.2012.36065.

[12] H. Mohammed, C. K. Jean, and W. A. Ahmad, “Projections of precipitation, air temperature and potential evapotranspiration in Rwanda under changing climate conditions,” *African J. Environ. Sci. Technol.*, vol. 10, no. 1, pp. 18–33, 2016, doi: 10.5897/ajest2015.1997.

[13] T. Yin *et al.*, “Impacts of climate change and human activities on vegetation coverage variation in mountainous and hilly areas in Central South of Shandong Province based on tree-ring,” *Front. Plant Sci.*, vol. 14, no. June, pp. 1–11, 2023, doi: 10.3389/fpls.2023.1158221.

[14] F. Ndayisaba, H. Guo, A. Bao, H. Guo, and F. Karamage, “Understanding the Spatial Temporal Vegetation Dynamics in Rwanda,” pp. 1–17, 2016, doi: 10.3390/rs8020129.

[15] E. Summary, “Rwanda Environment and Climate Change Analysis – Table of Contents,” pp. 1–26, 2019.

[16] REMA, “Rwanda State of Environment and Outlook,” *Minist. Nat. Resour.*, p. 98, 2009, [Online]. Available: http://www.rema.gov.rw/soe/

[17] P. Hawinkel, “Modeling vegetation dynamics driven by climate variability and land use changes in Rwanda,” no. Accomplished on March 2019, 2018.

[18] X. Zhou, L. Chen, J. Umuhoza, Y. Cheng, L. Wang, and R. Wang, “Intraseasonal oscillation of the rainfall variability over Rwanda and evaluation of its subseasonal forecasting skill,” *Atmos. Ocean. Sci. Lett.*, vol. 14, no. 6, p. 100099, 2021, doi: 10.1016/j.aosl.2021.100099.

[19] A. Mutabazi, “Rwanda Country Situational Analysis Climate Change Consultant Report, Camco, P.O. BOX 76406-00508, Nairobi, Kenya,” no. May, pp. 1–84, 2011.

[20] M. Cole, “Rwanda’s Climate : Observations and Projections,” no. July, p. 44, 2011.

[21] D. Ntwali, B. A. Ogwang, and V. Ongoma, “The Impacts of Topography on Spatial and Temporal Rainfall Distribution over Rwanda Based on WRF Model,” *Atmos. Clim. Sci.*, vol. 06, no. 02, pp. 145–157, 2016, doi: 10.4236/acs.2016.62013.

[22] C. B. Garrett, *Practical meteorology*, vol. s4-1, no. 55. 1858. doi: 10.1136/bmj.s4-1.55.57-b.

[23] L. G. Tanya Fuman, “Lesson 7 : Climates Of Africa - Forming Of The Sahara Desert Precipitation and

the Inter Tropical Convergence Zone (ITCZ)," *PenState Univ. E-ducation*, pp. 5–7, 2018.

[24] M. Newitt, "East Africa," *East Africa*, no. September, pp. 1–192, 2017, doi: 10.4324/9781315257167.

[25] K. Jonah *et al.*, "Spatiotemporal variability of rainfall trends and influencing factors in Rwanda," *J. Atmos. Solar-Terrestrial Phys.*, vol. 219, no. March, p. 105631, 2021, doi: 10.1016/j.jastp.2021.105631.

[26] T. Oakes, *Asia*. 2009. doi: 10.1016/B978-008044910-4.00250-9.

[27] P. I. Palmer *et al.*, "Drivers and impacts of Eastern African rainfall variability," *Nat. Rev. Earth Environ.*, vol. 4, no. April, 2023, doi: 10.1038/s43017-023-00397-x.

[28] R. Stull, *Chapter 4: Water Vapor*. 2015.

[29] B. Twinomugisha, U. Nations, and D. Programme, "Mapping the impacts of climate change in Eastern Rwanda Mapping the Impacts of climate change in Rwanda in target districts of Nyagatare , Kirehe , Gatsibo and Bugesera districts," no. July 2013, 2018.

[30] M. M. Mugunga, "Towards Improving the Skill of Seasonal Rainfall Prediction over Rwanda," 2019.

[31] P. Submitted, I. N. Partial, F. Of, and T. H. E. Requirements, "Association between madden-julian oscillations and wet and dry spells over rwanda," 2014.

[32] N. Etienne, "FUTURE RAINFALL PROJECTIONS FOR RWANDA USING STATISTICAL DOWNSCALING," 2018.

[33] F. Ntirenganya, "Analysis of Rainfall Variability in Rwanda for Small-scale Farmars Coping Strategies to Climate Variability," *East African J. Sci. Technol.*, vol. 8, no. 1, pp. 75–96, 2018.

[34] A. Ngabonziza, "COLLEGE OF SCIENCE AND TECHNOLOGY SCHOOL OF," 2022.

[35] J. Arnault and F. Roux, "Characteristics of African easterly waves associated with tropical cyclogenesis in the Cape Verde Islands region in July-August-September of 2004-2008," *Atmos. Res.*, vol. 100, no. 1, pp. 61–82, 2011, doi: 10.1016/j.atmosres.2010.12.028.

[36] MoE, "Rwanda Forest Cover Mapping," no. November, p. 235, 2019.

[37] M. Modeste, K. Abdellatif, M. Nadia, H. Zhang, U. M. V, and I. S. Rabat, "Open access impact of land

use and vegetation cover on risks of erosion in the Ourika watershed (Morocco),” *Am. J. Eng. Res. (AJER)*, vol. 5, no. 9, pp. 75–82, 2016, [Online]. Available: www.ajer.org

[38] S. S. da Cunha *et al.*, “Vegetation cover and seasonality as indicators for selection of forage resources by local agro-pastoralists in the Brazilian semiarid region,” *Sci. Rep.*, vol. 12, no. 1, pp. 1–10, 2022, doi: 10.1038/s41598-022-18282-w.

[39] S. N. Kane, A. Mishra, and A. K. Dutta, “Preface: International Conference on Recent Trends in Physics (ICRTP 2016),” *J. Phys. Conf. Ser.*, vol. 755, no. 1, 2016, doi: 10.1088/1742-6596/755/1/011001.

[40] F. N. Buba, E. N. Gajere, and F. F. Ngum, “Assessing the Correlation between Forest Degradation and Climate Variability in the Oluwa Forest Reserve, Ondo State, Nigeria,” *Am. J. Clim. Chang.*, vol. 09, no. 04, pp. 371–390, 2020, doi: 10.4236/ajcc.2020.94023.

[41] O. Report, “State of Environment and Outlook Report 2021,” 2021.

[42] R. Almalki, M. Khaki, P. M. Saco, and J. F. Rodriguez, “Monitoring and Mapping Vegetation Cover Changes in Arid and Semi-Arid Areas Using Remote Sensing Technology: A Review,” *Remote Sens.*, vol. 14, no. 20, 2022, doi: 10.3390/rs14205143.

[43] M. Ibrahim and A. Al-Mashagbah, “Change Detection of Vegetation Cover Using Remote Sensing Data as a Case Study: Ajloun Area,” *Civ. Environ. Res.*, vol. 8, no. 5, pp. 1–5, 2016.

[44] A. Sobieraj, “COMPARISON OF SEVERAL VEGETATION INDICES CALCULATED ON THE BASIS OF A SEASONAL SPOT XS TIME SERIES , AND THEIR SUITABILITY FOR LAND COVER,” no. 7, 2004.

[45] S. A. Hashemi, “Investigation of Relationship Between Rainfall and Vegetation Index by Using NOAA / AVHRR Satellite Images,” vol. 14, no. 11, pp. 1678–1682, 2011.

[46] A. Bannari, D. Morin, F. Bonn, and A. R. Huete, “A review of vegetation indices,” *Remote Sens. Rev.*, vol. 13, no. 1–2, pp. 95–120, 1995, doi: 10.1080/02757259509532298.

[47] A. E. Tengberg *et al.*, “The use of the Normalized Difference Vegetation Index (NDVI) to assess land degradation at multiple scales : a review of the current status , future trends , and practical considerations The use of the Normalized Difference Vegetation Index (NDVI) to ”.

[48] A. Ayanlade, “Remote sensing vegetation dynamics analytical methods: a review of vegetation indices techniques,” *Geoinformatica Pol.*, vol. 16, pp. 7–17, 2017, doi: 10.4467/21995923gp.17.001.7188.

[49] J. Cook, “Introduction to climate science denial,” *Res. Handb. Commun. Clim. Chang. Elgar Handbooks Energy, Environ. Clim. Chang.*, pp. 47–48, 2020, doi: 10.4337/9781789900408.00012.

[50] D. A. Dellasala and M. I. Goldstein, “Introduction: Climate Change,” *Encycl. Anthr.*, vol. 1–5, pp. xix–xx, 2017, doi: 10.1016/B978-0-12-809665-9.15009-8.

[51] H. Goosse, P. Y. Barriat, W. Lefebvre, M. F. Loutre, and V. Zunz, “Introduction to climate dynamics and climate modelling - Online Textbook,” *Online Textb. available Http//www.climate.be/textb.*, pp. 6–8, 2008, [Online]. Available: http://stratus.astr.ucl.ac.be/textbook/chapter5_node10.xml

[52] UNEP, “Climate Change 2023: Synthesis Report | UNEP - UN Environment Programme,” 2023, [Online]. Available: https://www.unep.org/resources/report/climate-change-2023-synthesis-report

[53] Intergovernmental Panel on Climate Change, *Climate Change 2021 The Physical Science Basis Summary for Policymakers Working Group I Contribution to the Sixth Assessment Report of the Intergovernmental Panel on Climate Change*. 2021.

[54] IPCC, “THE IPCC ’ S SIXTH ASSESSMENT REPORT Impacts , adaptation options and investment areas for a climate-resilient southern Africa,” 2021.

[55] G. Zhao, L. Ren, and Z. Ye, “Vegetation Dynamics in Response to Climate Change and Human Activities in a Typical Alpine Region in the Tibetan Plateau,” 2022.

[56] M. Lin, L. Hou, Z. Qi, and L. Wan, “Impacts of climate change and human activities on vegetation NDVI in China ’ s Mu Us Sandy Land during 2000 – 2019,” *Ecol. Indic.*, vol. 142, no. July, p. 109164, 2022, doi: 10.1016/j.ecolind.2022.109164.

[57] P. S. Loh, H. I. M. Alnoor, and S. He, “Impact of climate change on vegetation cover at south port sudan area,” *Climate*, vol. 8, no. 10, pp. 1–22, 2020, doi: 10.3390/cli8100114.

[58] L. Watershed, H. Khalis, A. Sadiki, F. Jawhari, H. Mesrar, and E. Azab, “Effects of Climate Change on Vegetation Cover in the Oued,” pp. 1–16, 2021.

[59] T. Ning, W. Liu, W. Lin, and X. Song, “NDVI Variation and Its Responses to Climate Change on the Northern Loess Plateau of China from 1998 to 2012,” vol. 2015, 2015.

[60] S. Hussain *et al.*, “Monitoring the Dynamic Changes in Vegetation Cover Using Spatio-Temporal Remote Sensing Data from 1984 to 2020,” 2022.

[61] U. K. M. Office, “Final Report : Rwanda Pilot”.

[62] V. Nzabarinda *et al.*, “Assessment and Evaluation of the Response of Vegetation Dynamics to Climate Variability in Africa,” pp. 1–22, 2021.

[63] J. M. Zúñiga-Vásquez, C. A. Aguirre-Salado, and M. Pompa-García, “Monitoring vegetation using remote sensing time series data: A review of the period 1996-2017,” *Rev. la Fac. Ciencias Agrar.*, vol. 52, no. 1, pp. 175–189, 2020.

[64] I. Aslanov, U. Mukhtorov, and R. Mahsudov, “Applying remote sensing techniques to monitor green areas in Tashkent Uzbekistan,” vol. 04012, pp. 10–14, 2021.

[65] FAO-FRA, “Fra 2000 Forest Cover Mapping & Monitoring With Noaa-Avhrr & Other Coarse Spatial,” *Work Pap.*, vol. 29, p. 42, 2000.

[66] D. Jacob *et al.*, “Assessing the transferability of the regional climate model REMO to different coordinated regional climate downscaling experiment (CORDEX) regions,” *Atmosphere (Basel).*, vol. 3, no. 1, pp. 181–199, 2012, doi: 10.3390/atmos3010181.

[67] A. Bartosova *et al.*, “Large-Scale Hydrological and Sediment Modeling in Nested Domains under Current and Changing Climate,” vol. 5, no. 5, pp. 1–13, 2021, doi: 10.1061/(ASCE)HE.1943-5584.0002078.

[68] R. Mpi-remo, “Change in Future Rainfall Characteristics in the Mekrou Catchment (Benin), from an Ensemble of,” 2008, doi: 10.3390/hydrology4010014.

[69] M. Déqué *et al.*, “A multi-model climate response over tropical Africa at +2 °C,” *Clim. Serv.*, vol. 7, pp. 87–95, 2017, doi: 10.1016/j.cliser.2016.06.002.

[70] C. Teichmann *et al.*, “How does a regional climate model modify the projected climate change signal of the driving GCM: A study over different CORDEX regions using REMO,” *Atmosphere (Basel).*, vol. 4, no. 2, pp. 214–236, 2013, doi: 10.3390/atmos4020214.

[71] M. I. Westphal, “Greenhouse Gas Emissions Scenarios: Background, Issues, and Policy Relevance,” p. 30, 2021, [Online]. Available: https://crsreports.congress.gov

[72] R. Moss *et al.*, *Towards New Scenarios for Analysis of Emissions, Climate Change, Impacts and Response Strategies*. 2008. [Online]. Available: http://www.osti.gov/energycitations/product.biblio.jsp?osti_id=940991

[73] A. Siebert *et al.*, "Evaluation of ENACTS-Rwanda: A new multi-decade, high-resolution rainfall and temperature data set—Climatology," *Int. J. Climatol.*, vol. 39, no. 6, pp. 3104–3120, 2019, doi: 10.1002/joc.6010.

[74] A. Kayiranga, F. Karamage, J. B. Nsengiyumva, and C. Mupenzi, "geosciences Analysis of Climate and Topography Impacts on the Spatial Distribution of Vegetation in the Virunga Volcanoes Massif of East-Central Africa," no. March, 2017, doi: 10.3390/geosciences7010017.

[75] S. Potithep, N. Nasahara, H. Muraoka, S. Nagai, and R. Suzuki, "What is the actual relationship between LAI and VI in a deciduous broadleaf forest? International Archives of the Photogrammetry," *Remote Sens. Spat. Inf. Sci. 38*, vol. XXXVIII, no. Vi, pp. 609–614, 2010.

[76] M. A. Worku and G. L. Feyisa, "Spatiotemporal dynamics of vegetation in response to climate variability in the Borana rangelands of southern Ethiopia," no. January, pp. 1–15, 2023, doi: 10.3389/feart.2023.991176.

[77] "DOWNSCALED CLIMATE PROJECTIONS FOR NATIONAL ADAPTATION PLAN IN RWANDA," no. May, 2022.

[78] B. Safari, J. N. Sebaziga, and A. Siebert, "Evaluation of CORDEX-CORE regional climate models in simulating rainfall variability in Rwanda," *Int. J. Climatol.*, vol. 43, no. 2, pp. 1112–1140, 2023, doi: 10.1002/joc.7891.

[79] R. K. Kaufmann *et al.*, "The effect of vegetation on surface temperature : A statistical analysis of NDVI and climate data," vol. 30, no. 22, pp. 3–6, 2003, doi: 10.1029/2003GL018251.

[80] G. Habiyaremye, J. De La, P. Mupenzi, and A. Karangwa, "Statistical Analysis of Climatic Variables and Prediction Outlook in Rwanda Statistical Analysis of Climatic Variables and Prediction Outlook in Rwanda," no. January, 2012.

[81] RESHU YADAV, S. K. TRIPATHI, G. PRANUTHI, and S. K. DUBEY, "Trend analysis by Mann-Kendall test for precipitation and temperature for thirteen districts of Uttarakhand," *J. Agrometeorol.*, vol. 16, no. 2, pp. 164–171, 2014, doi: 10.54386/jam.v16i2.1507.

[82] N. Kamal and S. Pachauri, “Mann-Kendall Test - A Novel Approach for Statistical Trend Analysis,” *Int. J. Comput. Trends Technol.*, vol. 63, no. 1, pp. 18–21, 2018, doi: 10.14445/22312803/ijctt-v63p104.

[83] F. Aswad, A. Yousif, and S. Ibrahim, “Trend Analysis Using Mann-kendall And Sen’s Slope Estimator Test for Annual And Monthly Rainfall for Sinjar District, Iraq,” *J. Univ. Duhok*, vol. 23, no. 2, pp. 501–508, 2020, doi: 10.26682/csjuod.2020.23.2.41.

[84] F. Aditya, E. Gusmayanti, and J. Sudrajat, “Rainfall trend analysis using Mann-Kendall and Sen’s slope estimator test in West Kalimantan,” *IOP Conf. Ser. Earth Environ. Sci.*, vol. 893, no. 1, 2021, doi: 10.1088/1755-1315/893/1/012006.

[85] M. Zimmerman, N. A. Peterson, and M. A. Zimmerman, “Beyond the Individual : Toward a Nomological Network of Organizational Empowerment Beyond the Individual : Toward a Nomological Network of Organizational Empowerment,” vol. 34, no. October 2004, 2016, doi: 10.1023/B.

[86] M. André, B. Vaz, and P. Santana, “Classification of the coefficient of variation to variables in beef cattle experiments,” no. 2002, pp. 9–12, 2017.

[87] S. Livingston, “Digital Commons @ DU Modeling Vegetation Cover at Mount St Helens Using Highly Correlated Vegetation Indices Modeling Vegetation Cover at Mount St Helens Using Highly Correlated,” 2022.

[88] N. R. J. Vol, R. Management, M. Regions, N. Resource, and E. Science, “Comparing Multiple Regression, Principal Componant Analysis, Partial Least Square Regression and Ridge Regression in Predicting Rangeland Biomass in the Semi Steppe Rangeland of Iran,” vol. 12, no. 1, pp. 1–21, 2014.

[89] B. Mahalingam, A. N. Deldar, and M. Vinay, “Analysis of Selected Spatial Interpolation Techniques for Rainfall Data,” *Int. J. Curr. Res. Rev.*, vol. 7, no. 7, pp. 66–71, 2015.

[90] D. Ozturk and F. Kilic, “Geostatistical approach for spatial interpolation of meteorological data,” *An. Acad. Bras. Cienc.*, vol. 88, no. 4, pp. 2121–2136, 2016, doi: 10.1590/0001-3765201620150103.

[91] Rwanda, “Climate Risk Country Profile:Rwanda,” *Rwanda 2006*, pp. 1–32, 2006, [Online]. Available: www.worldbank.org